TIDES STRUCTURES AND MIXING ALONG THE MOZAMBIQUE COAST

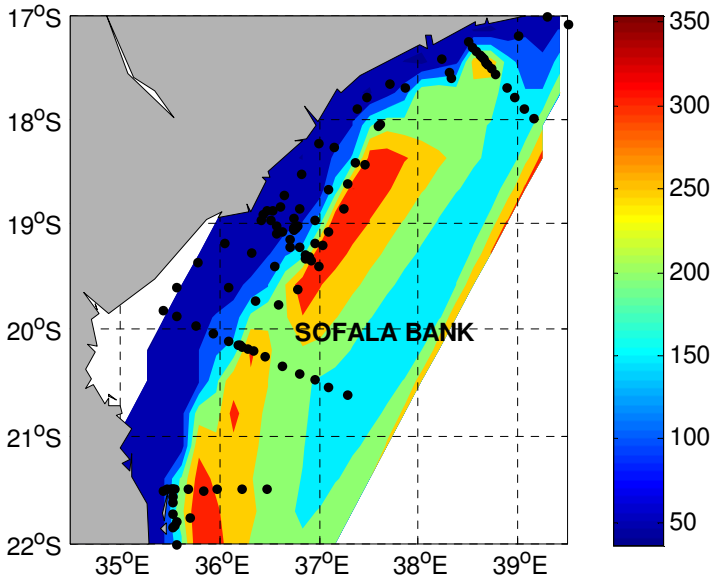

Cândida Inês Sete

NOMA Joint Master in Applied Marine Sciences

Supervisor: Tor Gammelsrød

Geophysical Institute, University of Bergen - Norway

June 2010

Acknowledgements

First of all, I wish to thankfulness to GOD who makes my dream realistic. I wish to show gratitude my supervisor Prof. Tor Gammelsrød for the helpful discussions, comments and support during the work on this thesis. I wish to thankful Dr. António Hoguane for the trust, the information and support assembled during this work. I am immensely thankful to the NOMA program for the scholarship received and the opportunity to study in Norway. I want to thank Kristin Kalvik and Marie Jones from Geophysical Institute at University of Bergen, to spend caring for all the bureaucratic details that made this possible. I am grateful to my colleagues at the Geophysical Institute, Valentina, Salma, Naftal, Jeremias, Elfatih, Waleed and Ahmed for their friendly and valuable help during the long- lasting semester. I am happy to have shared the snow and rain with all the students at Fantoft Student Hostel especially to Hellen Malebo, Marcia Pearson, Jabbie Kallon and Bachi for their friendly even far from Norway. Maybe we see each other some day again and go “shopping” together. I wish thank the kindergarten "Fantoft Gård Barnehage" to take care to my little girl Milena during my stay in Norway, particularly to Jannike Våge and Nathan the best friends of Milena. I appreciate all the time that Tone Slostvik spent to show me and Milena the tourists places in Bergen City. I wish to thank Noralf Slostvik and his family to show us Stavanger and to take caring my Milena when I was there. I wish to thank the Direction of INAHINA in particular for the Eng° Augusto Bata and dr. Cid Cambula for the time and bureaucratic details for the realization of this work. I want to thank dr. Sinibaldo Canhaga for the all support arranged during this work. I wish to thanks my Husband Adélio Nhapulo, my son Léslio Nhapulo and my daughters Denise Nhapulo and Milena Nhapulo for the moral support and patient during the realization of this work. I want to thank all family Sete, Munhequete, Cossa, Nhapulo, my grandmother Cândida Valoi, my brothers Manuel Sete and Lucas Sete and my sisters Adelina Maposse and Domingas Mavila specially my mother Laura Cossa and my father Domingos Sete who gave me the moral support along all years of my work. I wish to thank my friend Eugénia Mahumane who trusted me and helped me to solve some bureaucratic details to get authorization to Norway. Lastly I am grateful for many others have helped in different ways, and even though they might never know they did, I am deeply thankful.

Abstract

The resolution of environment problems suggests the study of tidal structures and mixing along the Mozambique Coast. Sofala Bank is the area with more available information for this study. Tides along the Mozambique Coast are semi-diurnal and tidal amplitudes vary over the year and in some location as Beira, achieve the amplitude of about 3.6 meters. The analysis of water level amplitudes reveals that it varies depending of location along the Mozambique Coast. Beira is the shallowest part of Mozambique Coast and is where the highest water level amplitude and the maximum dominating tidal component (M2) are found. The results indicate that tides along the Mozambican coast are standing waves. The application of the ROMS (Regional Ocean Model System) model results performs well the water level amplitudes. The study of currents shows the presence of stronger tidal current in Beira. The shallow areas along the coast are generally well mixed and around the shelf brake is developed stratification.

Contents

1. Introduction

Bathymetry

Mozambique is situated on the eastern coast of Southern Africa and has the third largest coastline in Africa (Sete, et al., 2002). Mozambique Channel is located between Madagascar on the east and Mozambique on the west, see Fig. 1.1. The bathymetry in Mozambique Channel is shown in Fig. 1.1. The south part has 4000 m depth, the north part with 3000 m and close to the coast of Mozambique and Madagascar the depth decreases from 2000 m to 500 m. We find shallow shelves less than 500 m and the widest are in the Sofala Bank, central part of Mozambique.

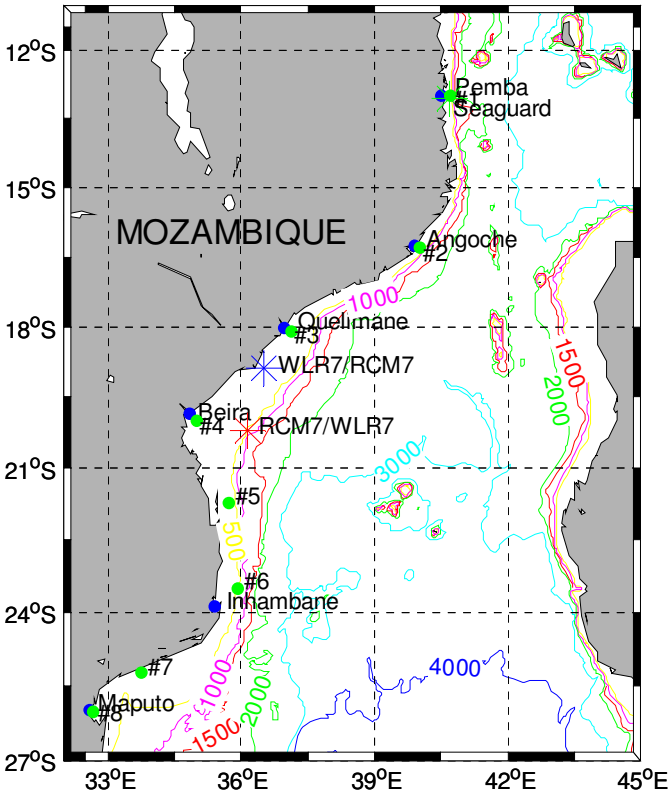

Figure 1.1: Bathymetry of the Mozambique Channel. Tide gauges and mooringspositions in Mozambique Coast. Legend: ● INAHINA's[1] tide gauge, moorings * RCM7/WLR7 (in November 1987), * WLR7/RCM7 (in February 1994), * Seaguard RCM (in November 2008) and ●# ROMS model stations.

[1] National Institute for Hydrograph and Navigation.

Currents

According to Sætre and Jorge da Silva (1982) the presence of cyclonic eddies seems that is associated with an inshore northward current, see Fig.1.2. Quartly and Srokosz (2003) using chlorophyll data from seaWiFs along Southern part of the Mozambique Channel concluded that the eastern side of the channel is mainly characterized by cyclonic eddies. Several of these cyclonic eddies then appear to move in west-southwesterly direction.

The geostrophic currents shown in Figure 1.2 which presents a large anticyclone eddy in central part (in Northern of the Mozambique Channel) between 16 º E and 18.5 º S, to the northeast and south of the anticyclone two cyclonic features is possible to see. The northeast cyclonic feature that is fairly uniformly circular, suggesting an eddy and to the south, the cyclonic feature is elongated, spreading across most of the channel. According to Kaehler, S. et al (2008) the current field is much more dynamic and turbulent, and seems to be eddy driven.

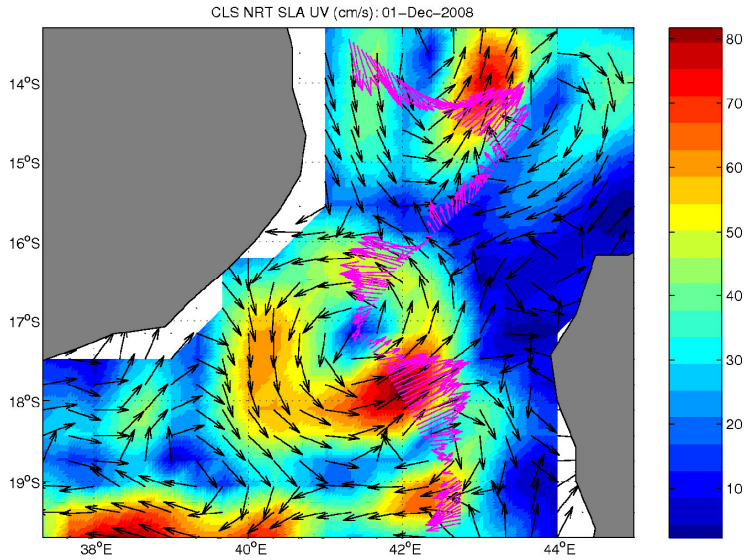

Figure 1.2: Eddies in Northern part of Mozambique. From Kaehler, S. et. al (2008); their figure 3.2.1.

The existence of spatial variations in flow velocity that is horizontal or vertical current shear commencing with small perturbations in the flow with a tendency to grow expanded into wave similar to patterns or eddies. The energy being removed from the mean flow is usually resulted by formation of eddies. The interaction between eddies often produces a complex patterns of eddies (Colling, 2001).

Tides

Tides are due to the gravitational attraction of the moon and sun. Monthly, the tides are affected by gravitational pull of the moon and the sun (Brown et al, 1999). According to Pugh (2004), tidal cycle occurs in an average of 12 hours and 25 minutes; consequently two tidal cycles occur every 24 hours 50 minutes (during roughly one day).The tides are classified by diurnal when they have a period of about one day (one high tide and one low tide daily); by contrast tides are semidiurnal when they occur twice daily (two high tides and two low tides each) (Pinet, 2006). The spring tides and neap tides are caused by the position of sun and moon around the earth. When the moon is full or new and the gravitational pull of the moon and sun are combined, the phenomena is called spring tide (at these times, the high tides are very high and the low tides are very low). Otherwise, when the gravitational forces of the Moon and the Sun are perpendicular to each other, the phenomena is called Neap tide (Brown et al, 1999). During the moon's quarter phases the effort of the sun and moon is at right angles, causing the bulges to cancel each other, see Fig.1.3. The result is a smaller difference between high and low tides. Neap tides are especially weak tides (Pinet, 2006).

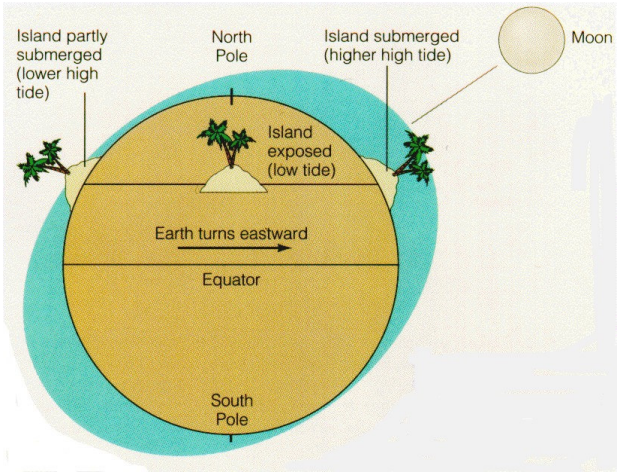

Figure 1.3: Rotation plane of the moon. From Garrison, T. (1996); his figure 11.11.

"*In most places the tidal range is typically of the order of few meters, and tidal ranges of more than about 10 m are known only at a few locations"* (Brown et al, 1999). Tidal range varies depending to location and can be reliably predicable because the cause of tidal wave motion is both continuous and regular (Brown et al, 1999). In the south central Indian Ocean there is an extensive region of large semidiurnal tides over which the phases change only

slowly (Pugh, 2004). Tides belong Mozambique Channel is known to be mainly semi-diurnal and in some location can achieve the amplitude of about 3.6 meters (see table 2.1).
The harmonic analysis provides the tidal constituents that are indispensable to predict the tide, see table 1.1.

Table 1.1: Some principal tidal constituents (Brown et al, 1999).

Name of tidal component	Symbol	Period in solar hours	Coefficient ratio (M_2 =10)
Principal lunar, semidiurnal	M_2	12.42	100
Pryncipal solar, semidiurnal	S_2	12.00	46.6
Principal lunar and solar, diurnal	K_1	23.93	58.4
Principal lunar, diurnal	O_1	25.82	41.5

Stratification and mixing

The river discharges along the Mozambique Coast have influence for the stratification. The mains rivers in Mozambique are showed in figure 1.4. Stratification depends on the rivers discharges (Pugh, 2004). Solar radiation, tides and wind are other factors that have influence in stratification ((Brown et al, 1999). Thermal and haline effects cause the stratification of the shelf seas (Simpson, 1998). The thermal structure of sea water is essential in order to understand the solar heating transfer between atmosphere and sea, as well as the transport of solar heating in the ocean and for comprehension of fisheries distribution and climatic analyze.

The currents in the water are generated by tides which interact with bottom producing turbulence. It tends to mix lower layers of water that may avoid any stratification and whole area may be permanently tidally mixed, if the current are sufficiently strong (Mann & Lazier, 2006). When tidal current are stronger, the front will move further offshore during spring tides and turbulent mixing can extend to the surface through a great depth of the water (Brown et al, 1999).

The turbulence transmits the wind effect downward to deeper layers (Colling, 2001). The vertical mixing of water column is caused by turbulence which is resulting from friction with the sea-bed. In areas where the water is shallow and the tidal currents are strong enough the vertical mixing of the water column is extended. In other areas where the water is deeper and the tidal currents are weaker, less mixing occurs, and stratification, with layers of different densities, can develop in summer when surface waters are warmed (Brown et al, 1999). In

stratified water column the organic matter dead due to the depleted of nutrients and sinks below the seasonal thermocline where take place the pycnocline (Brown et al, 1999).

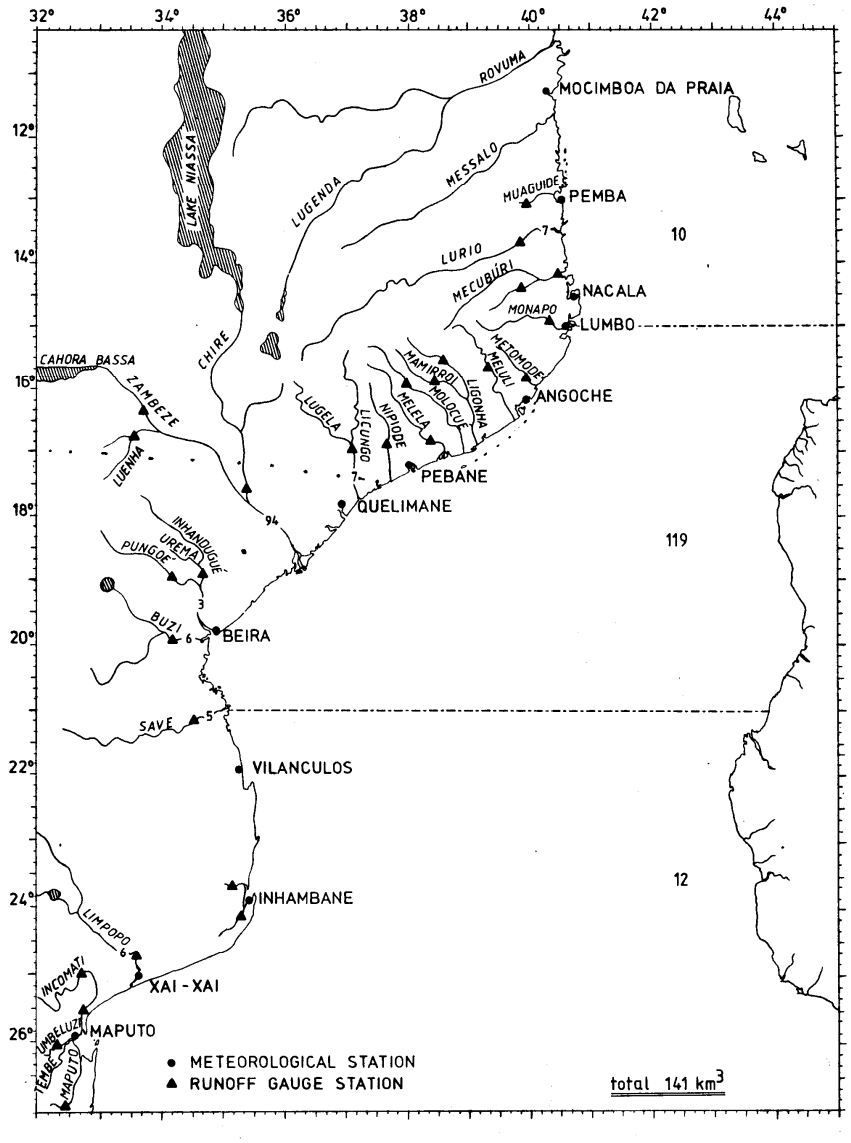

Figure 1.4: Location of the main rivers and mean annual freshwater runoff (Km^3) of Mozambique. From Sætre and Jorge da Silva (1982); their figure 6.

The salinity is important in determination of water masses movement, in circulation and other water properties, the quick renovation of the water. The salinity varies with river discharges (Lutjeharms, 2006b). The salinities of waters in the upper layers lie in a band between 35.00 and 35.40, with a few outliers, mostly as fresh water (Lutjeharms, 2006b). The trend for formation of cores layers of salinities and oxygen values has a relationship; the highest

salinity value core arises in the region of the lowest oxygen value (Sætre and Jorge da Silva, 1982).

Aim

The main objective of the study is to describe the tidal structures and mixing and to describe tidal currents along the Mozambique Coast. This information will be important to improve navigation and will contribute for a better comprehension of ecologic processes, to help in resolution of environment problems. An illustration of the application of the model result to study the mixing vs. stratification of the water column, and location of water front in Sofala Bank will be made.

2. Methods, Instruments and Data

2.1. Water level recorder (Tide gauges) from INAHINA

The Strip-Chart Water Level Recorder R20 (was located in Maputo, Quelimane and Pemba) and Horizontal Water Level Recorder Type X (Beira) is designed for the continuous recording of water level in stilling well and flowing waters (surface or ground water gauging). The recording accuracy in principle depends on size of the float, the recording ratio (height reduction), the arrangement of float cable (single or double cable run), and whether or not a reversal indicator is used. It is a pre-condition that the float movement is free, without any obstruction. The water level data was collected hourly. The instrument was made by OTT Hydrometrie, Germany.

Table 2.1: Tide gauge station (from INAHINA) and amplitude during extreme spring tides, see tide table (1995).

Station	Latitude	Longitude	Latitude (dms)	Longitude (dms)	Amplitude (m)
Pemba	-12.97	40.48	-12° 58' 00"	40° 29' 00"	2.3
Angoche	-16.23	39.9	-16° 13' 54"	39° 54' 06"	2.4
Quelimane	-18.00	36.97	-18° 00' 01"	36° 58' 12"	2.6
Beira	-19.82	34.83	-19° 49' 00"	34° 50' 00"	3.6
Inhambane	-23.87	35.37	-23° 52' 00"	35° 22' 36"	1.9
Maputo	-25.98	32.57	-25° 59' 00"	32° 34' 00"	2.0

Table 2.2: ROMS model station position and depths.

Station #	Depth (m)	Latitude (dms)	Longitude (dms)
1	914	-13° 00' 00"	40° 42' 00"
2	580	-16° 18' 00"	40° 00' 00"
3	30	-18° 06' 00"	37° 06' 00"
4	30	-20° 00' 00"	35° 00' 00"
5	521	-21° 42' 00"	35° 42' 00"
6	521	-23° 30' 00"	35° 54 00"
7	48	-25° 12' 00"	33° 45' 00"
8	30	-26° 00' 00"	32° 39' 00"

Table 2.3: Available information of water level from INAHINA.

Station	1995	1996	1997	1998	1999	2000	2001	2002	2003	2004	2005	2006	2007	2008	2009
Beira	A	A	A	A	A	A		C	C	C	C	C	C	C	C
Inhambane	B										A	A	A	A	A
Maputo	A	A	A	A	A	A	A	A	A	A	A	C	A	A	A
Pemba	A	A	A	A	A	A	A	A	A	A	A	A	A	A	A
Quelimane	A	A													

A - available, B – available but not all year C – available but still need to be validate.

2.2. Moorings (Current meters and tide gauge)

2.2.1. WLR7

The WLR7 is specially designed to measure ocean water levels. Placed on the seabed, the instrument records pressure and temperature. These parameters were recorded at regular intervals of time. On the basis of these data, precise variations in water level can be calculated. The instrument consists of a high precision quartz pressure transducer, an electronic board, a Data Storage Unit, wiring and hardware, all fastened to the top end plate and housed in a cylindrical pressure case. A measurement cycle, triggered by a high precision clock, starts with a forty seconds integration time of the pressure measurements. This eliminates pressure fluctuations due to waves. When the integration is completed, the data words are recorded. The data is stored in the Data Storage Unit (DSU) 2990, which is solid state memory. It also records the time of the first measurement and subsequently the time of every first measurement after midnight. The specifications are scheduled in the table 2.4. From http://www.oceanscan.net/db_documents/AANDERAAWLR7.PDF

A WLR7 was deployed at 200 m depth on 7 November 1987 to 16 November 1987 and another one was deployed at 25 m depth on 3 February 1994 to 16 February 1994 at Sofala

Bank location. For positions see map in Fig. 1.1 and for information about instrument depth see table 2.7. For this study pressure data was chosen to present as water level, subtracting the mean observed pressure.

Table 2.4: WLR7 specifications

Measures		
Temperature	Range	-3 to +35°C
	Accuracy	± 0.1°C
Pressure	Range	0 -700kPa (60m) (standard) 0 -3500kPa (340m) (standard)
	Accuracy	0.02% of full scale

2.2.2 RCM7

The Recording Current Meter (RCM7) is a self contained instrument that can be moored in sea and record ocean current (speed and direction), water temperature, conductivity of the water and instrument depth. The RCM7 consists of a recording unit and vane assembly which is equipped with a rod that can be mounted into the mooring line. A built-in clock triggers the RCM7 at present intervals and a total of six channels are sampled in sequence.

Table 2.5: RCM7 specifications

Measures		
Current speed	Range	2 to 295 cm/s
	Accuracy	±1 cm/s or ± 2%, whichever is greater
Current Direction	Range	0 - 360° magnetic
	Accuracy	± 5°
Temperature	Ranges	Low: - 2.46 to +21.48°C
		Wide: - 0.34 to +32.17°C
		High: 10.08 to +36.04°C
	Accuracy	± 0.05°C
	Optional Range	- 2.64 to +5.62°C (Arctic)

The channels represent a fixed reference reading for control purposes and data identification, measurement of temperature, conductivity, instrument's depth and the vector averaged current speed and direction respectively. The instrument records data internally and stored in Data Storage Unit (DSU) 2990. The output pulse keys on and off an acoustic carrier emitted by an acoustic transducer after simultaneous reading. The recording interval of the instrument is set by an interval selector switch. The sensor specifications for RCM7 are listed in the table 2.5.

After the retrieving of the mooring, the data stored in the Data Storing Unit could be read out as an ASCII format. From http://www.icsm.gov.au/tides/SP9/links/AanderaaRCM7.html.

One mooring was deployed at Sofala Bank in November 1987 for observation at 60 m and 170 m depth and another one was deployed in February 1994 for observation at 10 m and 20 m depth. For positions see map in Fig. 1.1 and for information about instrument depth see table 2.7.

The data were processed using the MATLAB program. The tide and current measurements were completed harmonic analysis by mean of T_tide software.

2.2.3. Seaguard RCM

Seaguard Recording Current Meter is based on the Seaguard datalogger platform and the ZPulse Doppler Current Sensor (rugged, true vector-averaging sensor for measuring current speed and direction in the sea, based on the backscatter acoustic Doppler principle) based on 300 pings.

Data storage takes place on a Secure Digital (SD) card. The current capacity for this card type is up to 4GBytes. The Seaguard also has a built-in power calculator which gives an estimated deployment length bases on selected interval. Battery type and current drain information, obtained from each smart sensor. The Seaguard RCM comes standard with the ZPulse multifrequency Doppler current sensor. The current sensor comprises acoustic pulses of several frequency components to lower the statistical variance in the Doppler shift estimate. The advantage of this is reduced statistical error with fewer pings, providing increased sampling speed and lower power consumption. The Doppler Current Sensor also incorporates a robust fully electronic compass and a tilt sensor.

The Seaguard RCM was also equipped with new smart sensor solutions for Temperature, Pressure and Conductivity.
From http://www.aadi.no/Aanderaa/Document%20Library/1/.../Seaguard®%20**RCM**.pdf

One Seaguard RCM was deployed at Pemba in November 2008 for observation at 800 m depth. For positions see map in Fig. 1.1 and for information about instrument depth see table 2.7.

Table 2.6: Seaguard RCM specifications

Measures		
Current speed	Range	0 to 300 cm/s
	Mean accuracy	± 0.15 cm/s
Current Direction	Range	0 - 360° magnetic
	Accuracy	± 5° ° for 0 - 15° tilt ±7.5° for 15 - 35° tilt
Temperature	Range	- 4 to +36°C
	Accuracy	± 0.03°C
Pressure	Range	0 -400kPa
	Accuracy	± 0,04% FSO
Conductivity	Range	0 – 7.5 S/m
	Accuracy	4319 A: ± 0.005 S/ 4319 B: ± 0.0018 S/m

Table 2.7: Mooring information.

Station	Instrument	Latitude (dms)	Longitude (dms)	Bottom depth (m)	Observation depth (m)	Start date	End date
Sof87	RCM7	-20° 13'	36° 09'	200	60	7/11/1987	13/11/1987
"	RCM7	-20° 13'	36° 09'	200	170	7/11/1987	16/11/1987
"	WLR7	-20° 13'	36° 09'	200	200	7/11/1987	16/11/1987
Sof94	RCM7	-20° 13'	36° 09'	25	10	3/02/1994	16/02/1994
"	RCM7	-18º 54'40"	36° 31'44"	25	20	3/02/1994	16/02/1994
"	WLR7	-18º 54'40"	36° 31'44"	25	25	3/02/1994	16/02/1994
Pemb08	Seaguard RCM	13º 04'	40° 42.3'	954	800	28/11/2008	28/12/2009

Table 2.8: Mean values from mooring observations.

Station	Instrument	Obs. depth (m)	Speed	U (cm/s)	V (cm/s)	T (°C)	S (psu)
Sof87	RCM7	60	40	25	20	20.4	35.25
"	RCM7	170	16	6	5	15.2	35.41
"	WLR7	200	-	-	-	14.2	-
Sof94	RCM7	10	27	-5	-6	28.5	35.27
"	RCM7	20	21	-4	-5	28.0	35.24
"	WLR7	25	-	-	-	27.6	-
Pemb08	Seaguard RCM	800	11	-1	-3	7.3	35.19

2.3. CTD

The main sensors of Seabird 911plus CTD are conductivity, temperature, pressure, and oxygen measurement at high accuracy. In order to achieve the highest possible accuracy the Sea-Bird 911 plus CTD incorporates certain key features like a fast and accurate single temperature sensor, a constant (pumped) flow without which the C and T sensors can not exhibit fixed time responses, a "TC Duct" to ensure that the conductivity and temperature sensors measures the same water and modular sensors permitting simple calibration and cross-checking.

Table 2.9: Seabird 911plus CTD specifications.

	Measurement Range	**Initial Accuracy**
Conductivity	0 to 7 Siemens/meter (0-70 mmho/cm)	0.0003 S/m (0.003 mmho/cm)
Temperature	-5 to +35 degC	0.002 degC
Pressure	Up to 15,000 Psia, depend. on configuration	0.015% of full scale
Dissolved oxygen	0-15 ml/l	0.1 ml/l

In order to enhance data integrity, raw data is acquired from the instruments and stored as raw unmodified data. A conversion program DATCNV uses the instrument configuration and calibration coefficients to create a converted engineering unit data file (.CNV) that is operated on by SEASOFT post processing modules. Each SEASOFT module that modifies the converted data file adds information to the header of the converted file permitting tracking of how the various oceanographic parameters were obtained.

Temperature and salinity measurements from Seabird 911 plus CTD along the Mozambique Coast were used to study oceanographic conditions. The CTD data were collected abroad at "Dr. Fridtjof Nansen" vessel at stations represented in figure 2.1, in October to November 2007.

The data were processed using the MATLAB program.

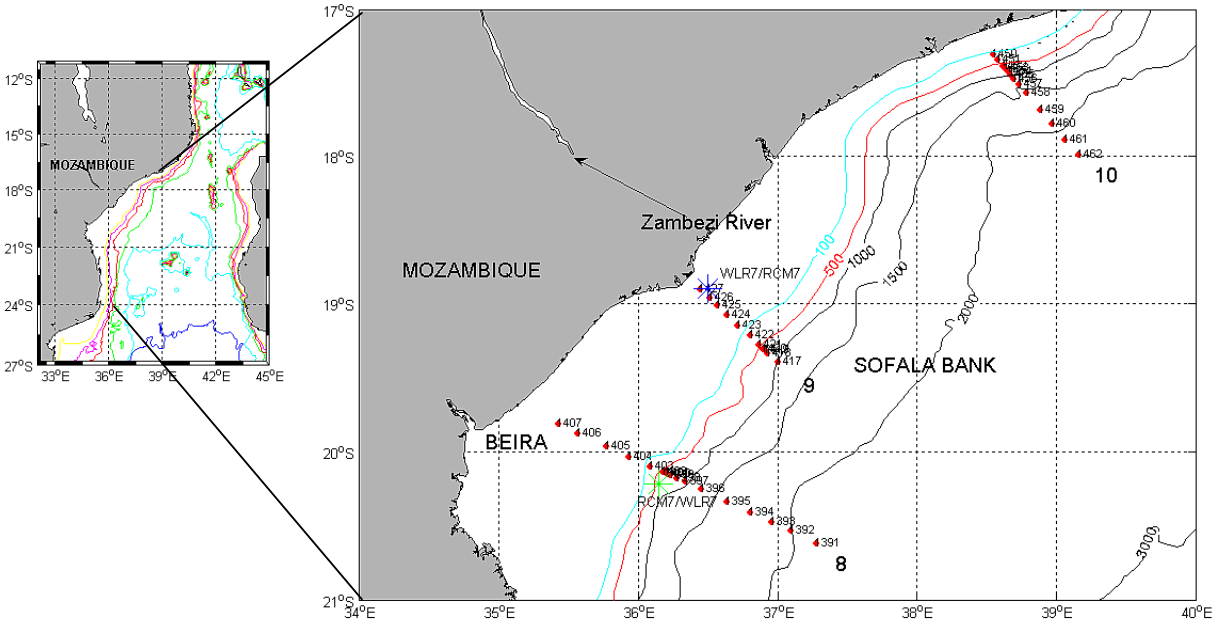

Figure 2.1: CTD stations and mooring positions at Sofala Bank in 2007.

2.4. ROMS Model

ROMS

The Regional Ocean Model System (ROMS) is a free-surface; hydrostatic, primitive equation ocean model that uses stretched, terrain-following coordinates in the vertical and orthogonal curvilinear coordinates in the horizontal. ROMS was completely rewritten to improve both its numeric and efficiency in single and multi-threaded computer architectures. It also was expanded to include a variety of new features including high-order advection schemes; accurate pressure gradient algorithms; several sub grid-scale parameterizations; atmospheric, oceanic, and benthic boundary layers; biological modules; radiation boundary conditions; and data assimilation. ROMS has been intended to be a multi-purpose, multi-disciplinary oceanic modeling tool. From http://www.ess.co.at/ICZM/roms.html.

According to Segtnan (2006), the model was run by Paul Budgell at the Institute of Marine Research in Bergen, for the year 2002. Two different runs were performed with different conditions at the open boundaries. The model covers the Mozambique Channel and the region around Madagascar. Model fields were stored as daily means and the model station every hour, see table 2.2.

The horizontal axes are denoted ζ and η (Fig. 2.2). To keep high resolution in the entire model domain, resolution is equal everywhere. It then follows that ζ and η can not be east-north coordinates. However, because the domain is so limited in size, the north and east axes are considered to be straight lines. The north and east component of ζ and η are then found by means of the angle between the north axis and the ζ axis (Segtnan, 2006).

According to Segtnan (2006) in the vertical, ROMS uses stretched, terrain-following coordinates. Terrain-following coordinates (σ) are calculated as follows:

$$\sigma = \frac{z - \zeta}{H + \zeta} \quad (2.1)$$

where ζ is the surface elevation, z is the altitude depth and H is the equilibrium depth. σ goes from -1 (bottom) to 0 (surface), and is divided into 30 layers, where layer number 30 is the surface layer (referred to as σ layer 30).

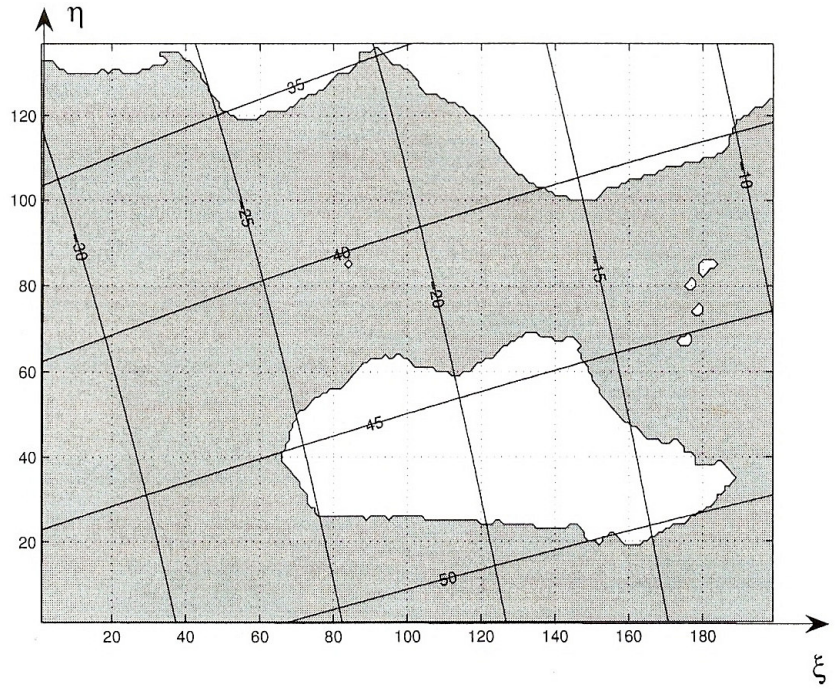

Figure 2.2: Model domain: ξ and η denotes the axes of model grid points. Latitudes and longitudes are drawn. From Segtnan (2006); her figure 2.

For better resolution in the areas of interest, such as at the thermocline and at the bottom boundary layers, stretched coordinates are introduced z is then calculated as:

z = Hc . σ + (H - Hc) .Sc (2.2)

where Sc is the stretched coordinates, one for each σ layer. The critical depth, i.e. the minimum depth in the region is represented by Hc and is equal to 10 m (Segtnan, 2006).

Regional Ocean Model System (ROMS) results were evaluated touching data obtained from tide gauges (from INAHINA) and moorings (WLR7, RCM7 and Seaguard RCM) located along the Mozambique Coast, see table 2.2 and 2.3. The ROMS model data were available for the period 1995 – 2005. For this study we used the data of 1995, 1996, 1997 and 2000. The model period does not coincide with WLR7, RCM7 and Seaguard RCM. For analyze of tides and tidal currents we compared INAHINA's and mooring harmonic constituents with model, see table 3.2, 3.3 and 3.4. We chose the period of November 1987 for Sofala 87 mooring, February 1994 for Sofala 1994 mooring and 28th November to 13rd December 2008 for Pemba 2008 mooring for the tidal analysis in order to calculate tidal ellipses.

3. Results

3.1 Water level

Some examples of water level recording along the Mozambique Coast are shown in Fig. 3.1. The amplitude is about 1.5 m in Maputo, 3 m in Beira, 2 m in Quelimane and Pemba. The comparison of water level along 16 days for Maputo, Beira, Quelimane and Pemba (see Fig. 3.1 b) illustrates the difference in amplitude. The amplitude is high in Beira and is followed by Quelimane, Pemba and Maputo (small). The phase it seems equal for all stations; the high and low water level happens at almost same time at four locations. To looks for the differences in phase we compare observed water level for Maputo, Beira, Quelimane and Pemba during 2 days, see Fig. 3.1 c). The water level data were collected hourly. There is the difference of amplitude for all locations. Maputo and Beira demonstrates some delay relatively Quelimane and Pemba. The water level reaches at first Pemba followed by Quelimane, Maputo and Beira.

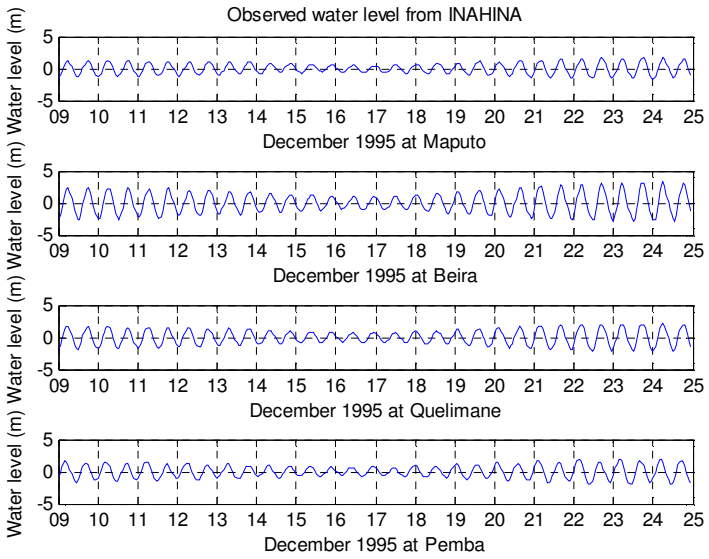
Observed water level from INAHINA
Water level (m)
December 1995 at Maputo
December 1995 at Beira
December 1995 at Quelimane
December 1995 at Pemba

a)

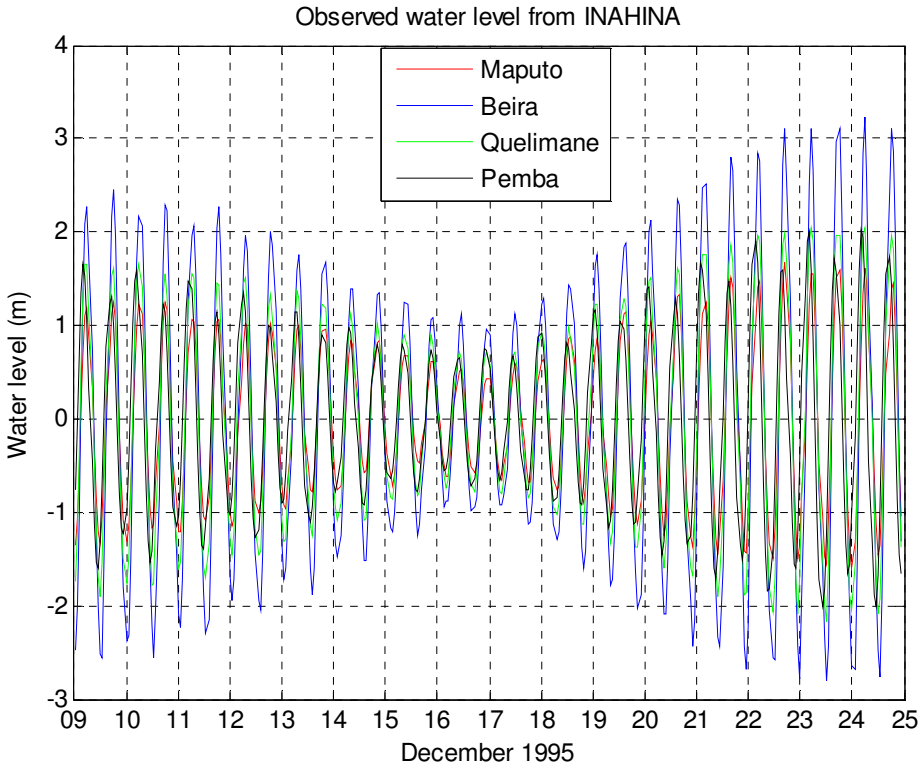
Observed water level from INAHINA
Maputo
Beira
Quelimane
Pemba
Water level (m)
December 1995

b)

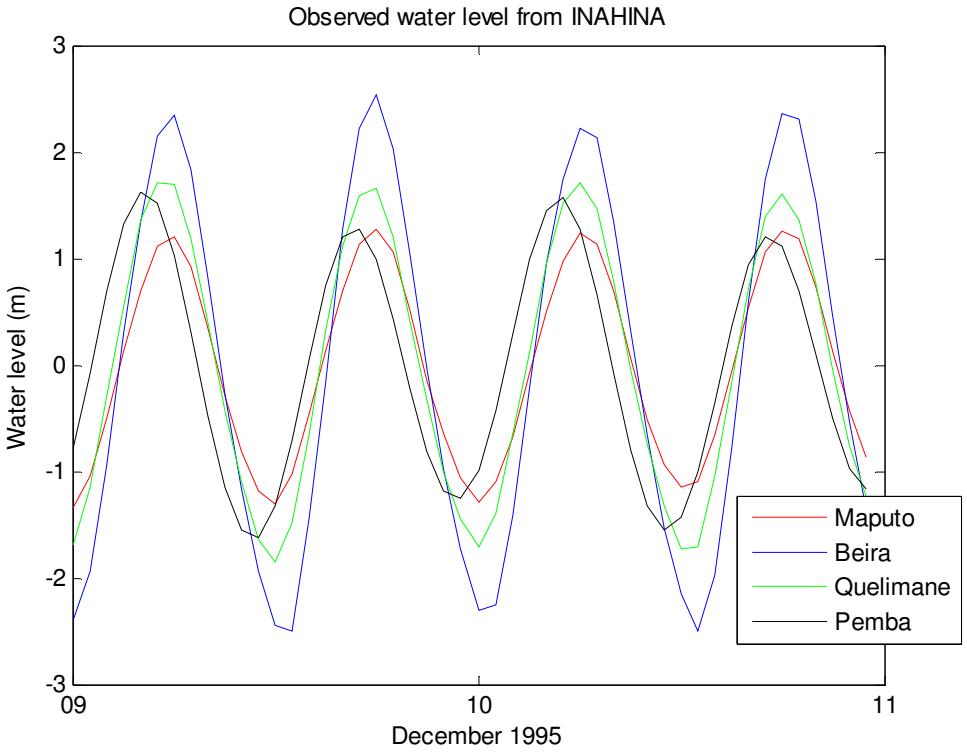

c)

Figure 3.1: a) Observed water level from INAHINA, b) Comparison of observed water level from INAHINA, 16 days and c) Comparison of observed Water level from INAHINA, 2 days.

3.2. Comparison of observation and model

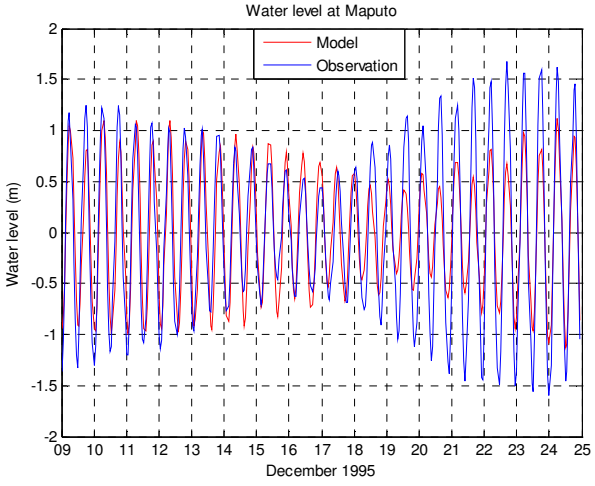

a)

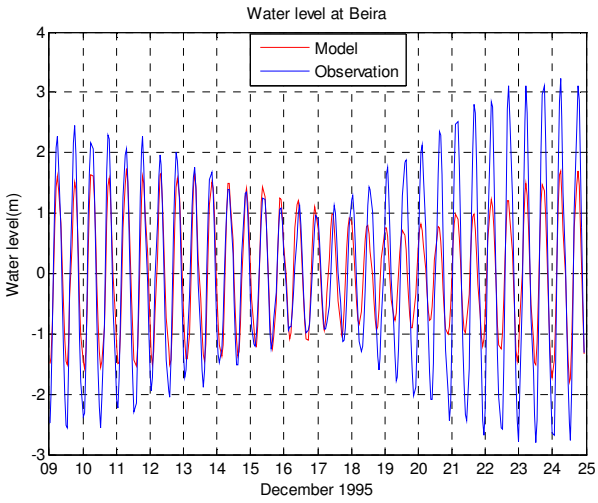

b)

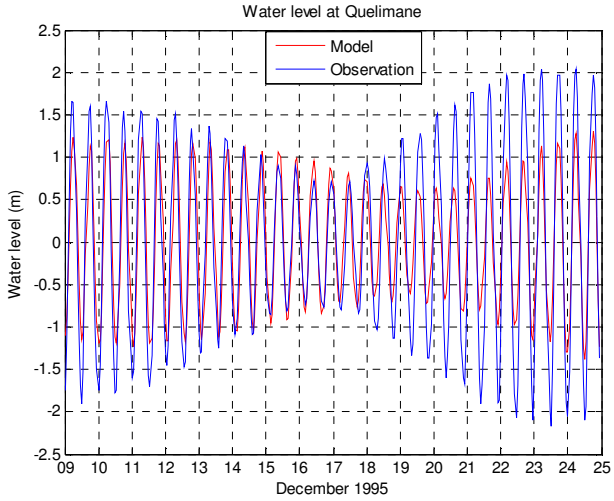

c)

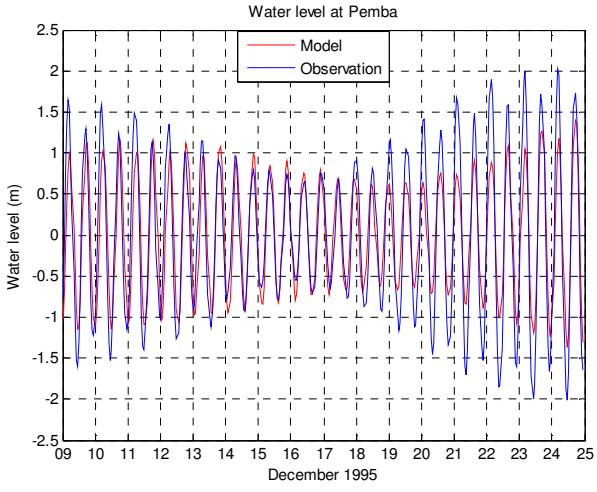

d)

Figure 3.2: Observed and modeled water level at Maputo (a), Beira (b), Quelimane (c) and Pemba (d).

The observed water level and modeled water level from Maputo, Beira, Quelimane and Pemba are shown in Fig. 3.2. The observed amplitudes of water level in four places are high than the model amplitudes, up to a factor 2 at Beira, see table 3.1. Note that for the diurnal variation in the M2 signal at Maputo (Fig 3.2 a) where the model seems to be out of phase with the observations.

Table 3.1: Observed and modeled water level amplitude during extreme spring water level.

Station	**Amplitude (m)**	
	Observation	**Model**
Maputo	1.5	1
Beira	3	1.5
Quelimane	2.2	1.3
Pemba	2	1.3

3.3. Observations from moorings

Sofala Bank 1994

The observations of water level, u, v, temperature and salinity at 10m and 20m depth are represented in Fig. 3.3, see also table 2.8 for average values. The water level amplitude is almost 2 m, see Fig. 3.3 a. The current speed (Fig. 3.3 b and c) presents a tidal signal. If we see the current variation at 10m and 20m depth, it varies from north-east until around 8th February, and south-west until around 14th February and back again to north-east. During spring tide we can see that the current varies from south-west. The maximum temperature is almost 29.5 °C at 10 m and 29 °C at 20 m depth. When the current is south-west the temperature is high and back to low when the current is north-west at 10 m and 20 m depth. The salinity shows the jump for high salinities when the temperature is high at 10 m and 20 m depth. The maximum salinity is around 35.5 psu at 10 m and 20 m depth.

Sofala Bank 1987

The observations of water level, u, v, temperature and salinity at 60 m and 170 m depth are represented in Fig. 3.4, see also table 2.8 for average values. The water level amplitude is almost 1.5 m, see 3.4 a). The current speed (Fig. 3.4 b and c) presents a tidal signal. Due to the current meter fault the available information refers short time (around five days) for 60 m depth. The current at 60 m depth varies from north-east during all period and at 170 m depth varies from south-west until around 12th November and north-east in rest of days. The

temperature at 60 m depth shows a tidal signal and at 170 m depth when the current changes to south-west the temperature become high. The salinity at both depth (60 m and 170 m) shows a stationary variation from about 35.2 psu to 35.4 psu depth and from 35.3 psu to 35.5 psu at 60 m and 170 m depth respectively. There is a tidal signal in temperature and not in salinity.

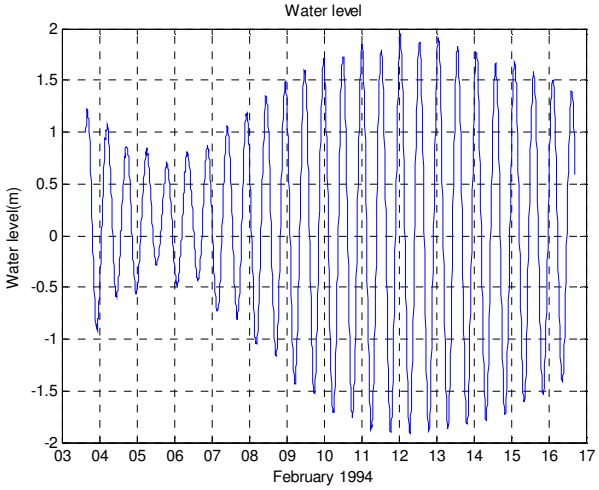

a) 25 m

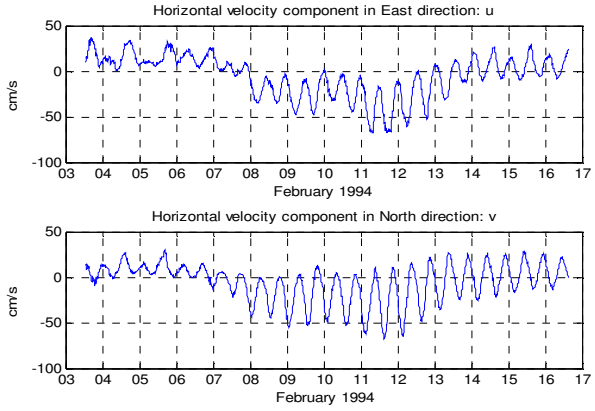

b) 10 m

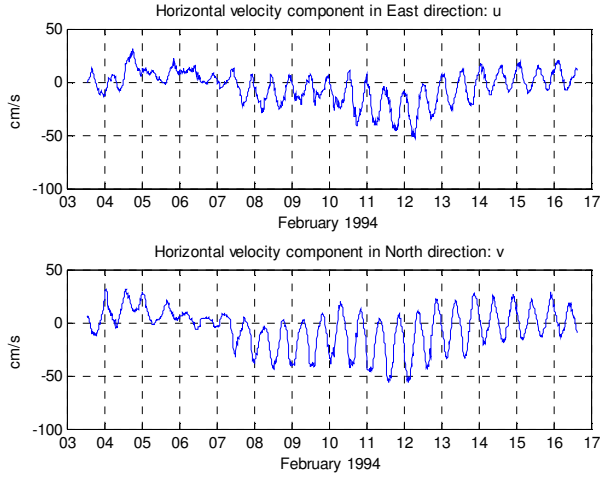

c) 20 m

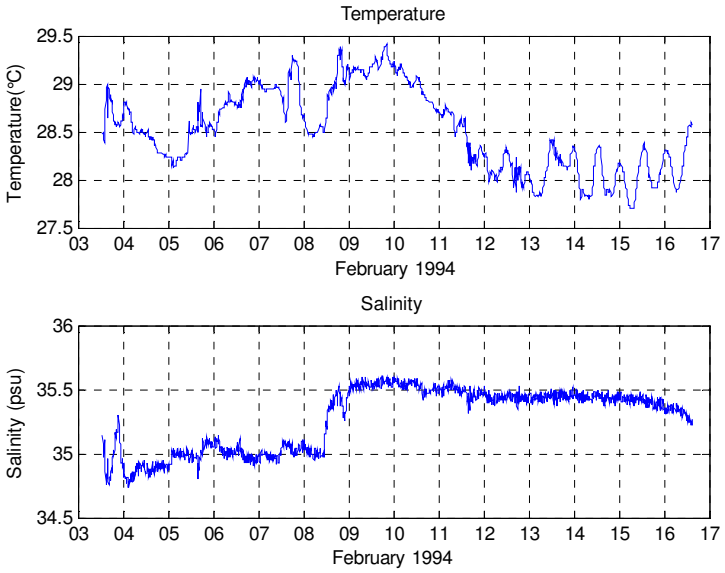

d) 10 m

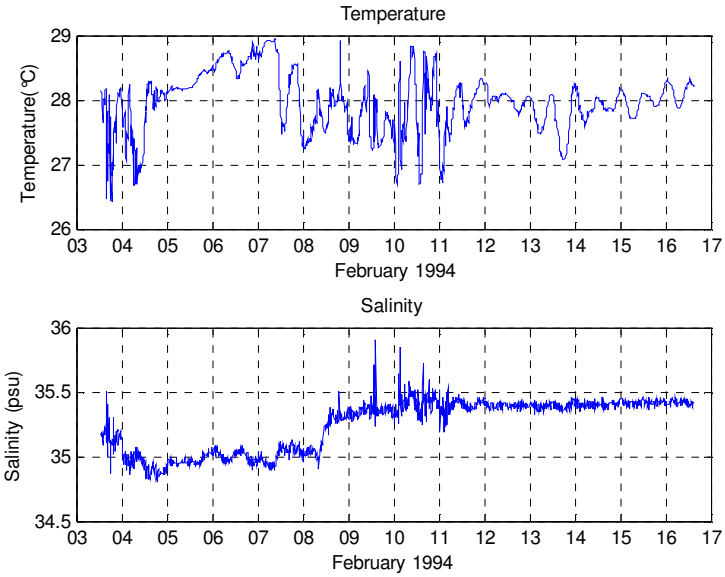

e) 20 m

Figure 3.3: Observations from mooring at Sofala 1994 a) water level at 25 m, b) u and v at 10m, c) u and v at 20m, d) temperature and salinity at 10m and e) temperature and salinity at 20m.

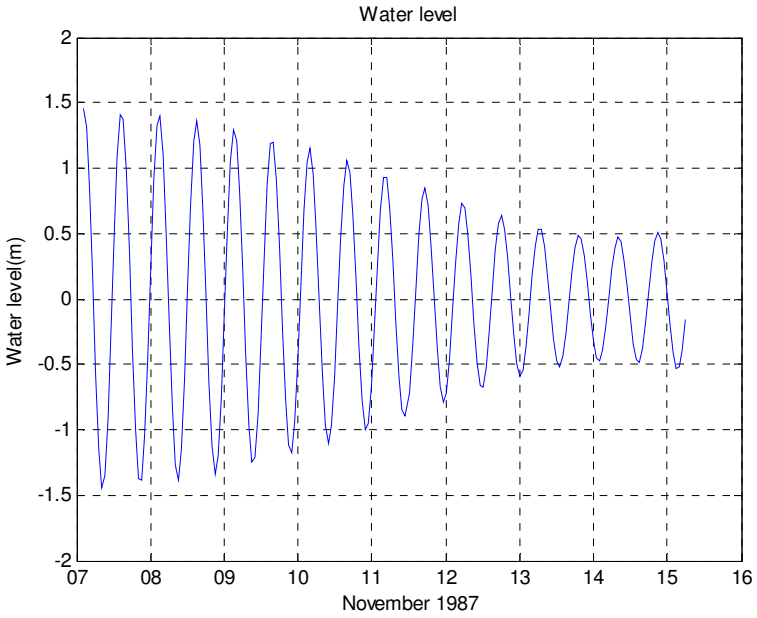

a) 200 m

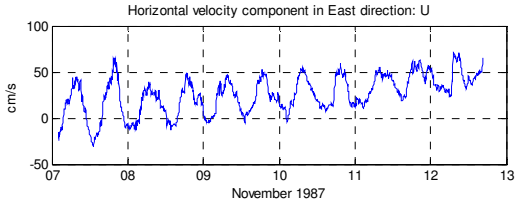

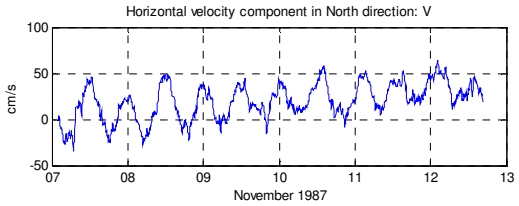

b) 60 m

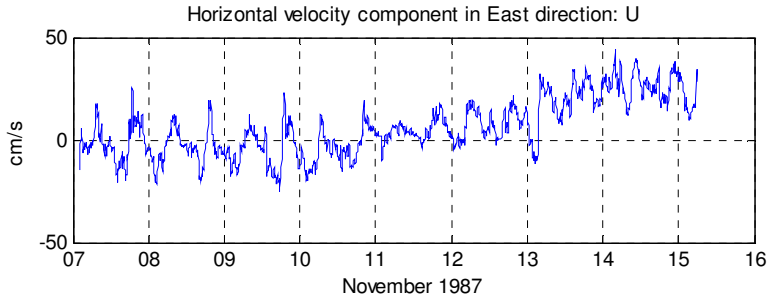

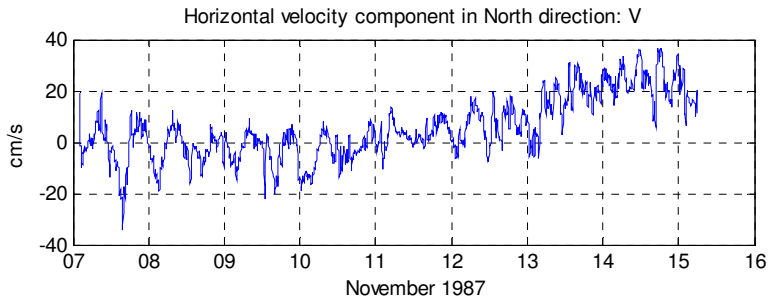

c) 170 m

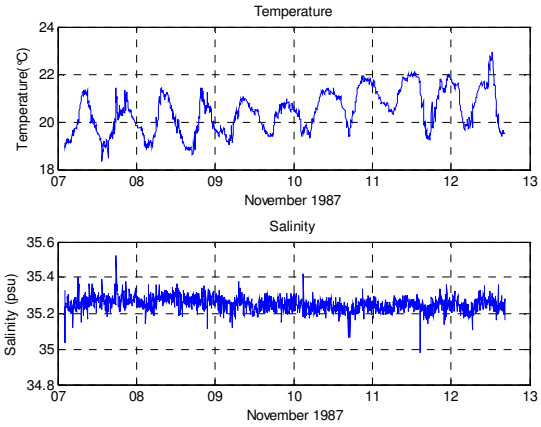

d) 60 m

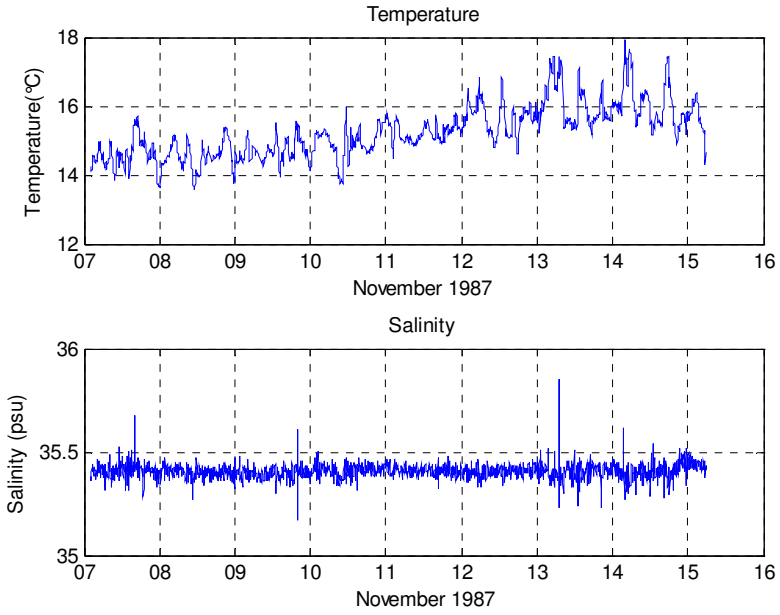

e) 170 m

Figure 3.4: Observations from mooring at Sofala Bank 1987 a) water level at 200 m, b) u and v at 60m, c) u and v at 170 m, d) temperature and salinity at 60 m and e) temperature and salinity at 170 m.

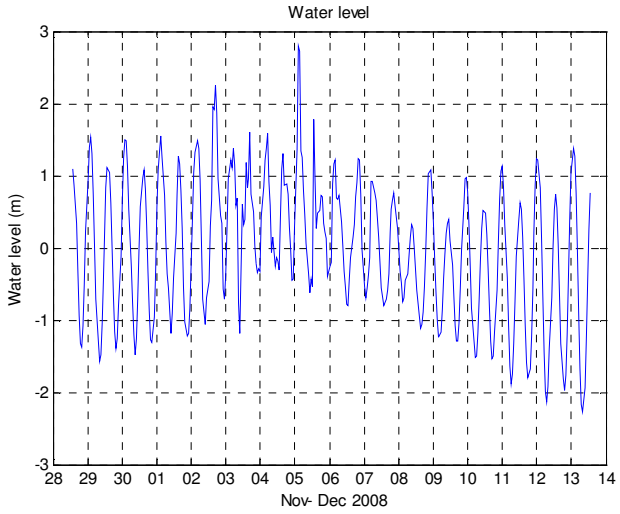
Water level
Water level (m)
3
2
1
0
-1
-2
-3
28 29 30 01 02 03 04 05 06 07 08 09 10 11 12 13 14
Nov- Dec 2008

a)

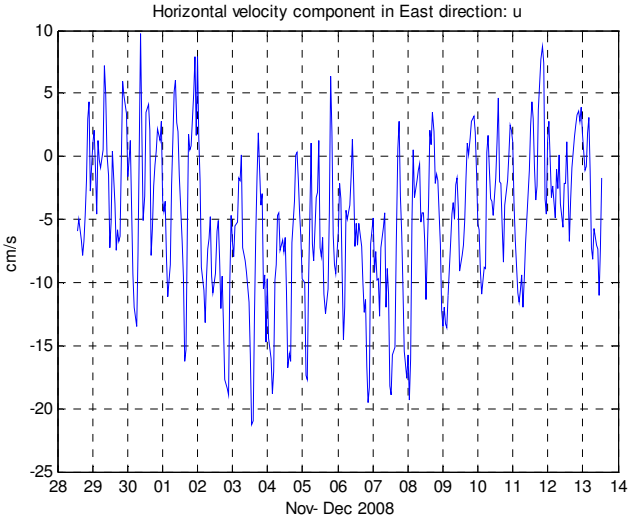
Horizontal velocity component in East direction: u
cm/s
10
5
0
-5
-10
-15
-20
-25
28 29 30 01 02 03 04 05 06 07 08 09 10 11 12 13 14
Nov- Dec 2008

b)

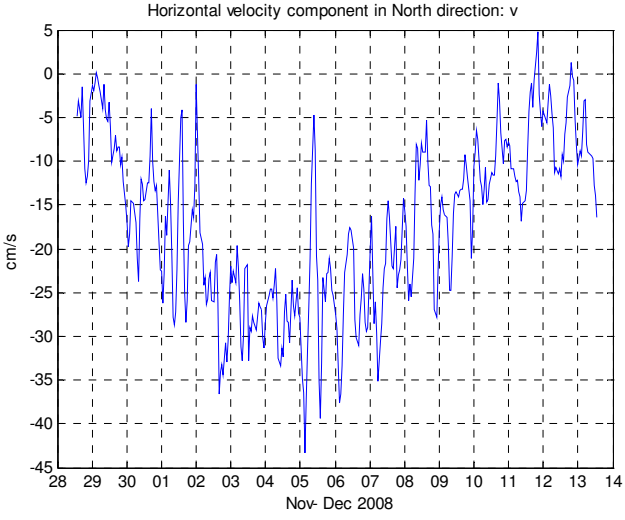
Horizontal velocity component in North direction: v
cm/s
5
0
-5
-10
-15
-20
-25
-30
-35
-40
-45
28 29 30 01 02 03 04 05 06 07 08 09 10 11 12 13 14
Nov- Dec 2008

c)

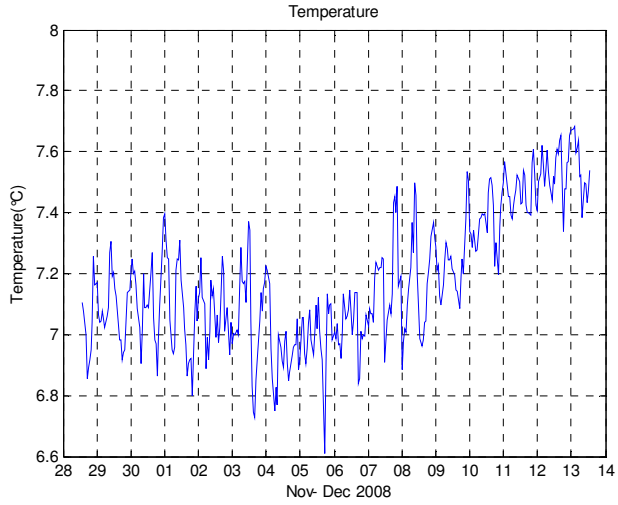

d)

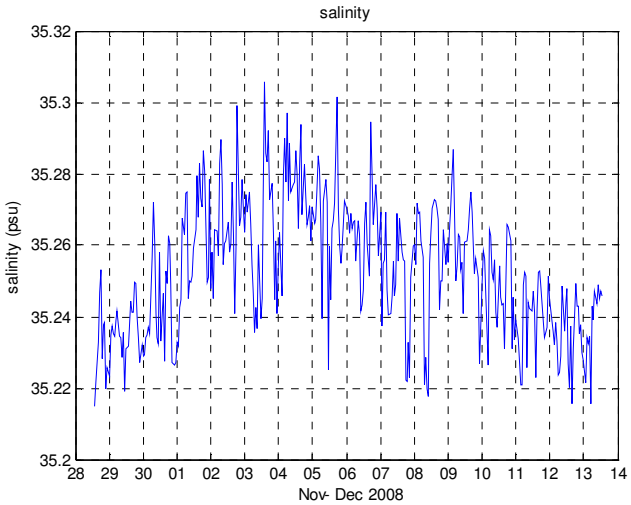

e)

Figure 3.5: Observations from mooring at Pemba 2008, 800 m a) water level, b) u, c) v d) temperature e) salinity.

Pemba 2008

The observations of water level, u, v, temperature and salinity at 800 m depth are represented in Fig. 3.5, see also table 2.8 for average values. The water level amplitude is about 2 m, see 3.5 a). The current speed (Fig. 3.5 b and c) presents a tidal signal. The current (u) is mainly negative and (v) is almost always negative, so the direction is South- south west during all period. The temperature shows variation between 6.8 °C to 7.4° C at first days and start to increases from about 8th December until the end of the days to about 7.6 °C. There is a tidal signal in temperature. During the variation of current South south-west, the salinity increases to about 35.30 psu until 4th December and decreases to about 35.22 psu in rest of days.

3.4. Comparison of mooring and model

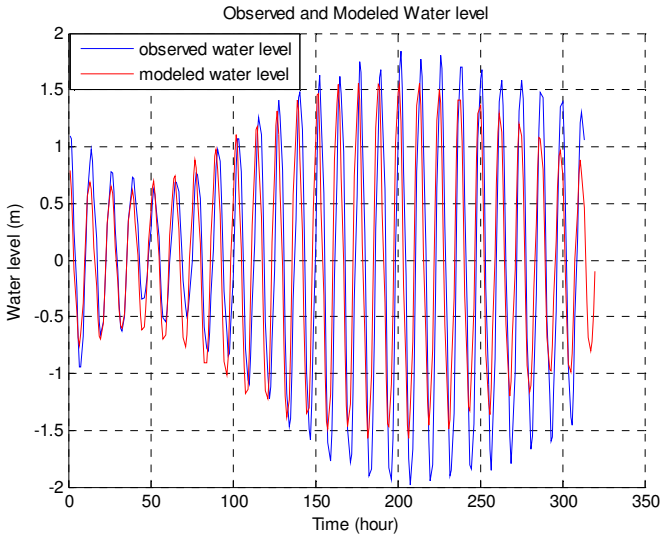

Figure 3.6: Observed (3 to 16 February 1994) and model (22 February to 5 March 1995) water level at Sofala Bank.

Due to the lack of model data from 1994 for the comparison was used the information of 1995, presented in Fig. 3.6. The model shows the same structure of water level although the model presents smaller amplitudes than observations, low to a factor 1.3. The observed and modeled water level is referred to different periods but the moon phase is chosen to be the same (third quarter moon). The spring and neap tide happen at same time for observed and modeled water level.

3.5. Tidal constituents

The observed and model amplitude of tides is shown in table 3.2. The tide O1, K1, M2 and S2 presents higher amplitude for observation than in the model for all station (Maputo, Beira, Quelimane and Pemba) except in Maputo and Beira which K1 demonstrates higher amplitude for model than observation. Looking at the observed and modeled amplitude, Beira presents the biggest M2 following by Quelimane, Pemba and Maputo.

The observed and model amplitude from for moorings are shown in table 3.3 for water level and 3.4 for currents. The WLR7 at Sofala 94 presents the bigger amplitude of M2 than the rest of places. The RCM7 at Sofala 87 presents the bigger amplitude of M2 comparing with another location in the table 3.3.

Table 3.2: Harmonic constituents for Maputo and model (#8) from 1 January to 31 January 2000, Beira and model (#4) from 4 May to 3 June 1996, Quelimane and model (#3) from 19 May to 2 June 1995 and Pemba and model (#1) from 18 May to 1 June 1997 .

INAHINA Station	**Tide**	**Amplitude (m)**		**Phase (deg)**	
		Observation	**Model**	**Observation**	**Model**
Maputo	O1	0.03	0.01	339	11
	K1	0.06	0.09	243	107
	M2	0.98	0.72	118	72
	S2	0.48	0.32	169	241
Beira	O1	0.05	0.02	18	216
	K1	0.04	0.05	63	121
	M2	1.81	1.42	99	269
	S2	0.90	0.57	166	218
Quelimane	O1	0.05	0.03	50	273
	K1	0.05	0.05	31	295
	M2	1.30	0.95	122	173
	S2	0.55	0.37	151	192
Pemba	O1	0.09	0.02	30	153
	K1	0.14	0.04	21	334
	M2	1.19	0.83	80	73
	S2	0.47	0.39	114	49

Table 3.3: Harmonic constituents for observation (WLR7 and seaguard RCM) and model (#3, #4 and #1) data.

Station	**Mooring**	**Bottom depth (m)**	**Tide**	**Amplitude (m)**		**Phase (deg)**	
				Obs.	Model	Obs.	Model
Sof87	WLR7	200	K1	0.02	0.06	332	6
			M2	0.94	1.10	29	16
Sof94	WLR7	25	K1	0.03	0.04	75	15
			M2	1.22	0.86	170	13
Pemb08	Seaguard RCM	954	K1	0.21	0.04	358	201
			M2	0.96	0.82	43	356

Table 3.4: Harmonic constituents for observation (RCM7 and seaguard RCM) and model (#3, #4 and #1) data.

Station	**Mooring**	**Obs. Depth (m)**	**Tide**	**Major axis (cm/s)**		**Minor axis (cm/s)**		**Inclination (deg)**		**Phase (deg)**	
				Obs.	Model	Obs.	Model	Obs.	Model	Obs.	Model
Sof87	RCM7	60	K1	4	1	-1	0	78	45	131	314
			M2	25	10	9	-0	132	165	316	276
"	RCM7	170	K1	1	0	0	-0	176	137	106	249
			M2	4	10	1	0	33	165	176	282
Sof94	RCM7	10	K1	4	2	-2	1	18	73	330	3
			M2	18	6	-13	3	99	168	242	293
"	RCM7	20	K1	2	1	0	0	87	21	48	61
			M2	18	6	-9	3	108	166	224	297
Pemb08	Seaguard RCM	800	K1	1	1	0	0	93	133	257	115
			M2	2	6	1	2	155	44	203	170

3.6. Temperature, Salinity, Sigma-T and Oxygen

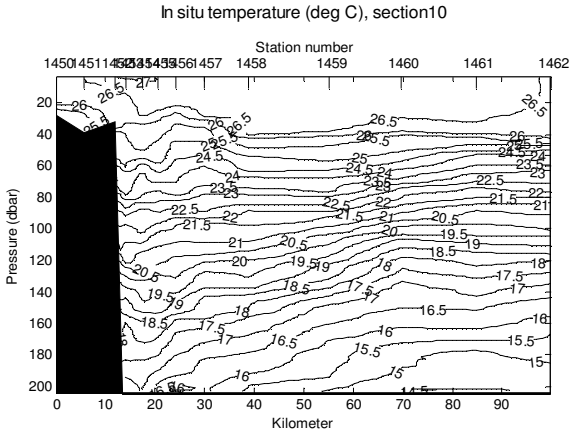

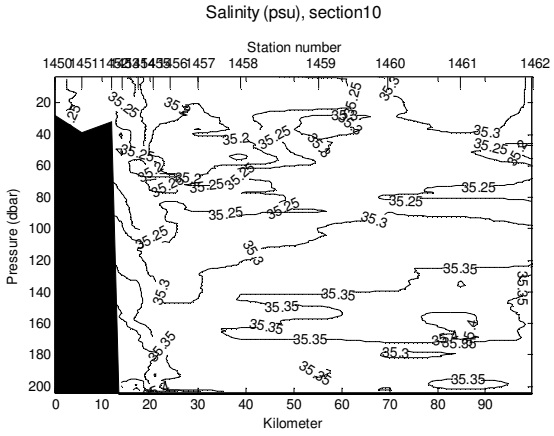

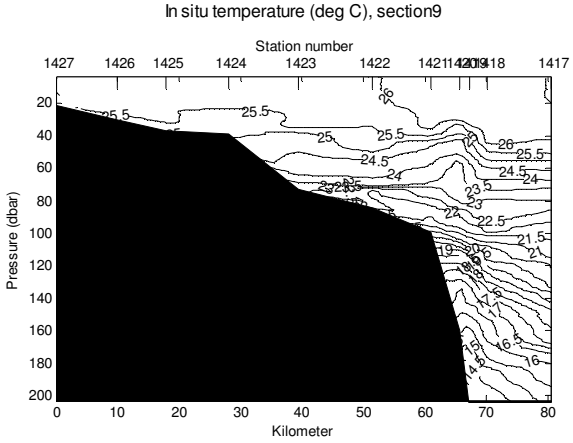

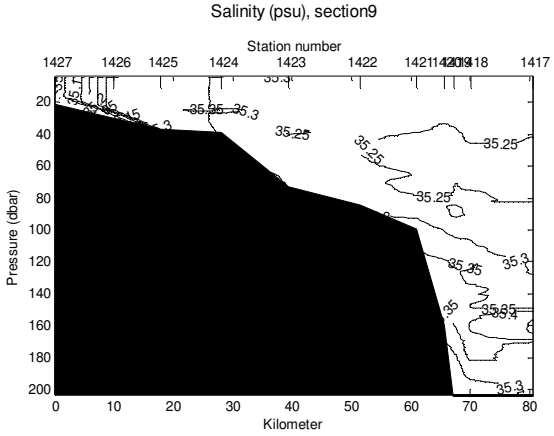

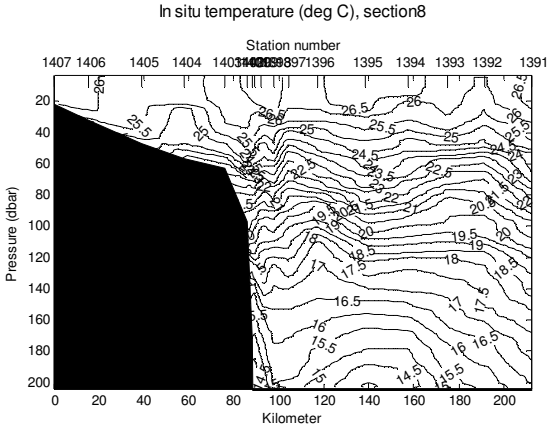

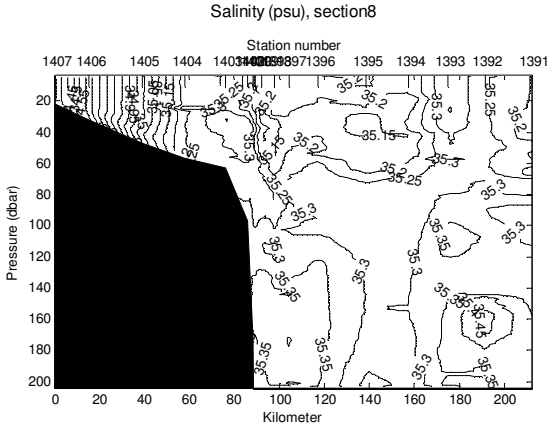

(a) (b)

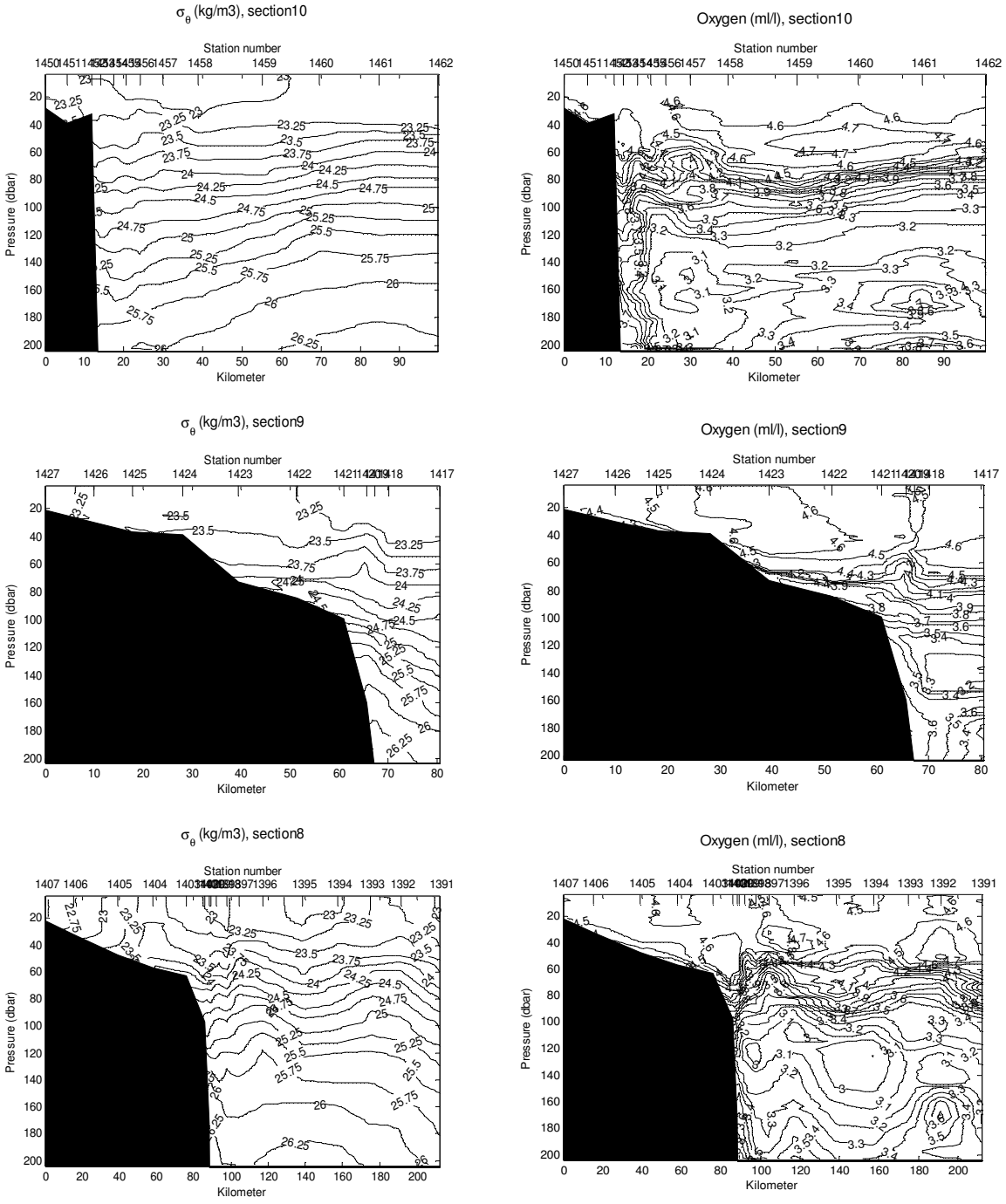

(c) (d)

Figure 3.7: CTD section plots for section 10 (upper), 9 (middle) and 8 (lower). (a) Temperature, (b) Salinity, (c) Sigma-T and (d) Oxygen. Sofala Bank in September to October 2007, see Fig. 2.1 for positions.

The temperature, salinity, sigma-T and Oxygen plots of CTD section 8, 9 and 10 are shown in Fig. 3.7. The temperature in all section is warm at surface, which is around 26.5 ºC and is quite constant in the upper 40 m. The thermocline is found at about 80 – 100 m depth. The salinity shows a more patchy structure with maximum salinities almost as high as 35.5 psu. Note the influence of the brackish water on the shelf particularly in section 8 and 9. That the isohalines are vertical indicate a strong mixing on the shelf, more pronounced at section 8. The density has roughly the same structure as the temperature, indicating that the temperature is dominating the density. The Oxygen in section 10 decreases (4.6 ml/l to 3.2 ml/l) from about 20 m to 120 m depth and increases (3.2 ml/l to 3.8 ml/l) from about 140 m to 200 m depth but close to the coast there is a horizontal gradient which presents the decreasing from the coast to the sea. It is not uniform in all layers, at about 160 m depth there is a core of 3 ml/l (low oxygen) close to the coast and other core of 3.7 ml/l at the sea part (high oxygen). In section 9 the oxygen shows horizontal gradient from about 0 m to 60 m depth and from about 140 m to 200 m depth; and vertical gradient from 60 m to 120 m with decreasing structures. In section 8, the oxygen gradient is vertical from 40 m to 100 m and there are cores along water column from surface to 60 m depth and 120 m to 180 m depth. The region where are formed the cores of high salinities values there are cores formation of low oxygen values.

4. Discussion

4.1. Water level

The water level reaches at first Pemba followed by Quelimane, Beira and Maputo according to Fig. 3.1c. It is probably due to the fact that Pemba is located at open sea part of Mozambique Coast. The amplitude for Sofala Bank mooring showed in figure 3.3 and 3.4 denotes that the water level close to the coast, at 25 m depth (RCM9 in 1994) has bigger amplitude (2 m) than at 200 m depth (RCM7 in 1987) which is 1.5 m. The big amplitude may be due to the fact that the mooring and Beira station is located in shallow part of Mozambique Coast. Another possibility is that Beira presents different topography with sand banks, there is situated the Sofala Bank.

According to table 3.1, Beira has the biggest observed and modeled amplitude during extreme spring water level, follow by Quelimane, Pemba and Maputo. This result is same comparing with INAHINA's table (2.1).

From the pressure measurements obtained at Pemba, (Fig. 3.5a) it was difficult to find the exact water level amplitude during spring tide may be because the calculated mean sea level for all values was zero, although at end the water level oscillates in different position between 0.5 m. When the current speed is strong the mooring is tilted. Since the Seaguard was located at 154 m above the bottom (see table 2.7), only a very slight tilt is necessary to explain the increase in the pressure corresponding to an increase in the water level increase of around 1- 2 m (see fig. 3.5 b and c).

We made an effort to show how the ROMS model performed at the Sofala 94 mooring when it comes to water level. For this analyze was chosen a period of 1995 from the model since ROMS model observations are not available for 1994. The period with the same moon-phase (third quarter moon) was selected careful in 1995. The comparison is shown in Fig.3.6. The result shows that the observed water level amplitude and phase are coincident with model, although the ROMS model amplitudes are smaller than the observed, low to factor of 1.3. The ROMS model performed well.

4.2. Tidal constituents

According to Pugh (2004), there is the need of at least 14.77 days of length of data available to separate M2 and S2 and it was proved by harmonics analysis (table 4.1). For the case of WLR7 deployed at Sofala Bank in 1987 and 1994, was possible to separate only the constituents K1 and M2 which are two of some principal tidal constituents see table 2.1. The data length of water level available was 8 days (1987) and 13 days (1994) instead of 14.77 days which is necessary to separate M2 and S2. The result of harmonic analysis for observation and model data is shown in table 3.2 that the amplitudes and phase for observation and model water level presents difference. The observed and modeled amplitude for Beira presents the biggest M2 following by Quelimane, Pemba and Maputo, see table 3.2.

Tidal constituents in Mozambique Channel are semidiurnal. According to Pugh (2004), Pond, S. and Pickard, G. (1983), the form factor is the relation between the sums of diurnal amplitudes by the sum of semidiurnal amplitudes of tides, equation (4.1).

$F = \dfrac{AK_1 + AO_1}{AM_2 + AS_2}$ (4.1) (from Pugh (2004); his formula 3.7). Where A is tidal amplitude.

$F_{Pemba} = 0.14$, $F_{Quelimane} = 0.05$, $F_{Beira} = 0.03$ and $F_{Maputo} = 0.06$

In the case of Pemba, Quelimane, Beira and Maputo the form factor was situated between 0 and 0.25 (from table 3.2) that proves the fact that the tide is semidiurnal, according Pugh (2004).

If we see the figure 3.2a, there is the difference in phase between observation and model for Maputo station, the modeled amplitude is in phase, but diurnal constituent K1 seems to be 180º out of phase. In accordance of the table 3.2 which shows that K1 of the model is 136 º out of phase (which is far from 180 º). But 136 º is still closer to 180º than 0.

4.2.1. Tidal ellipses

The tidal ellipses of M2 and K1 components for Sofala bank and Pemba are shown in Fig. 4.1, 4.2 and 4.3. According to Fig. 4.1, M2 at 60 m depth presents a bigger major axis (25 cm/s) than observed at 170 m depth. The tidal ellipse orientation of M2 is anti-clockwise. From Fig. 4.2 tidal ellipses for M2 at 10 m and 20 m depth presents almost the same major axis and inclination angle for observation, see also table 3.4. The tidal ellipse orientation of M2 is clockwise. M2 at 800 m depth presents the small major axis (2 cm/s), see Fig. 4.3 and table 3.4. The tidal ellipse orientation of M2 is anti-clockwise. After analyses of the observation results, we notice that at 60 m depth the dominating M2 component has the biggest major axis of tidal ellipse comparing with other (10 m, 20 m, 170 m and 800 m) depth. If we compare the observation and model ellipses, we found that there is difference between observation and model that shows the big major axis for observation except at 170 m and 800 m depth, which the observation has small major axis than model, see Fig. 4.1, 4.2 and 4.3; and also table 3.4. The observations and model tidal constituents refer different period, although the tidal ellipse orientation of M2 are not bad comparing observation (1987, 1994 and 2008) and model (1995). The model shows difference in tidal ellipse orientation of M2 for Sofala 94, which is clockwise, see Fig. 4.2. From Fig. 4.1 the model shows the collapse of the tidal ellipses caused by minor axis (zero). It seems that when the minor axis is zero the ellipse degenerate in a straight line.

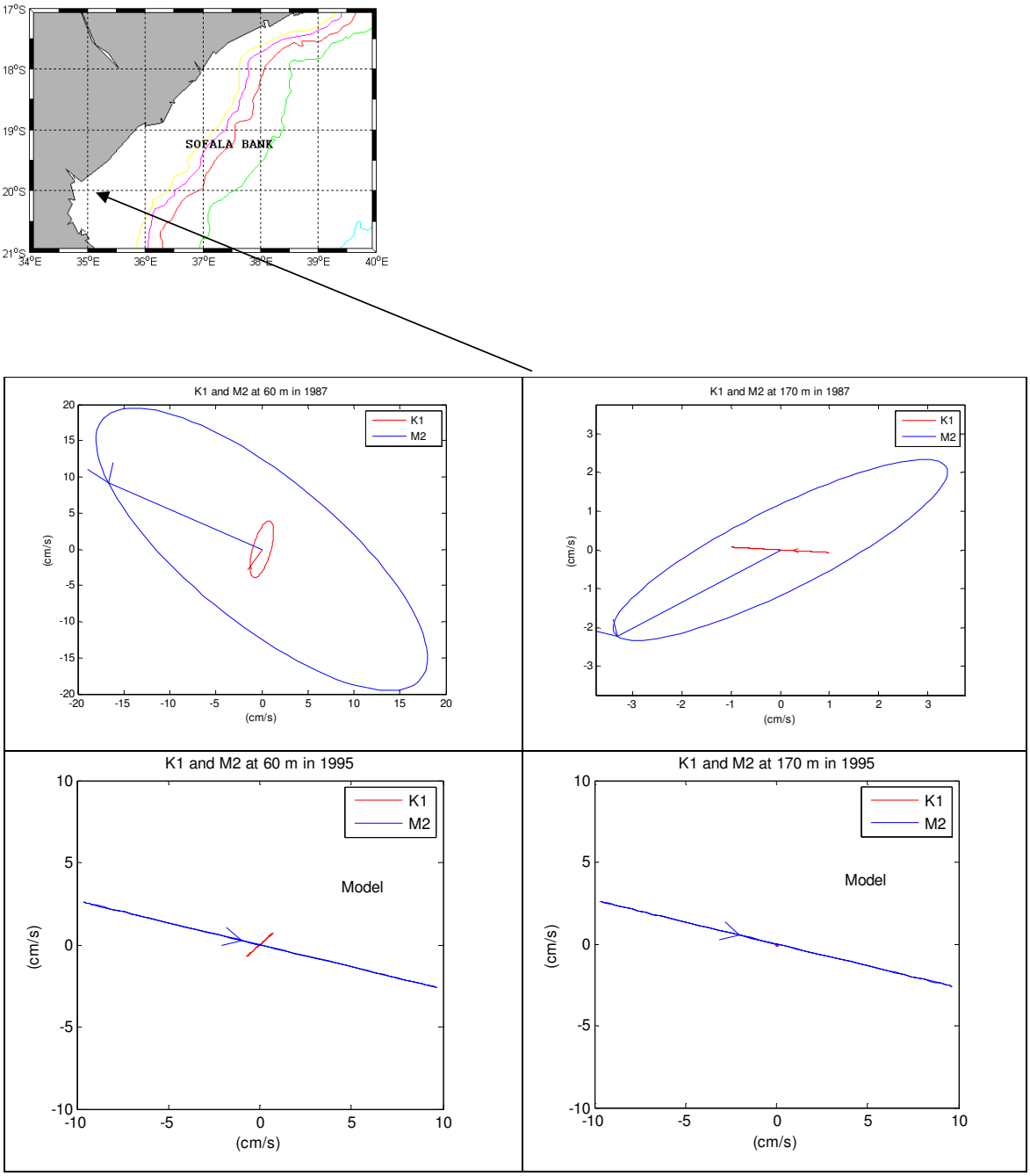

Figure 4.1: Tidal ellipses for K1 and M2 constituents observed (1987) and modeled (1995) at Sofala 87 location.

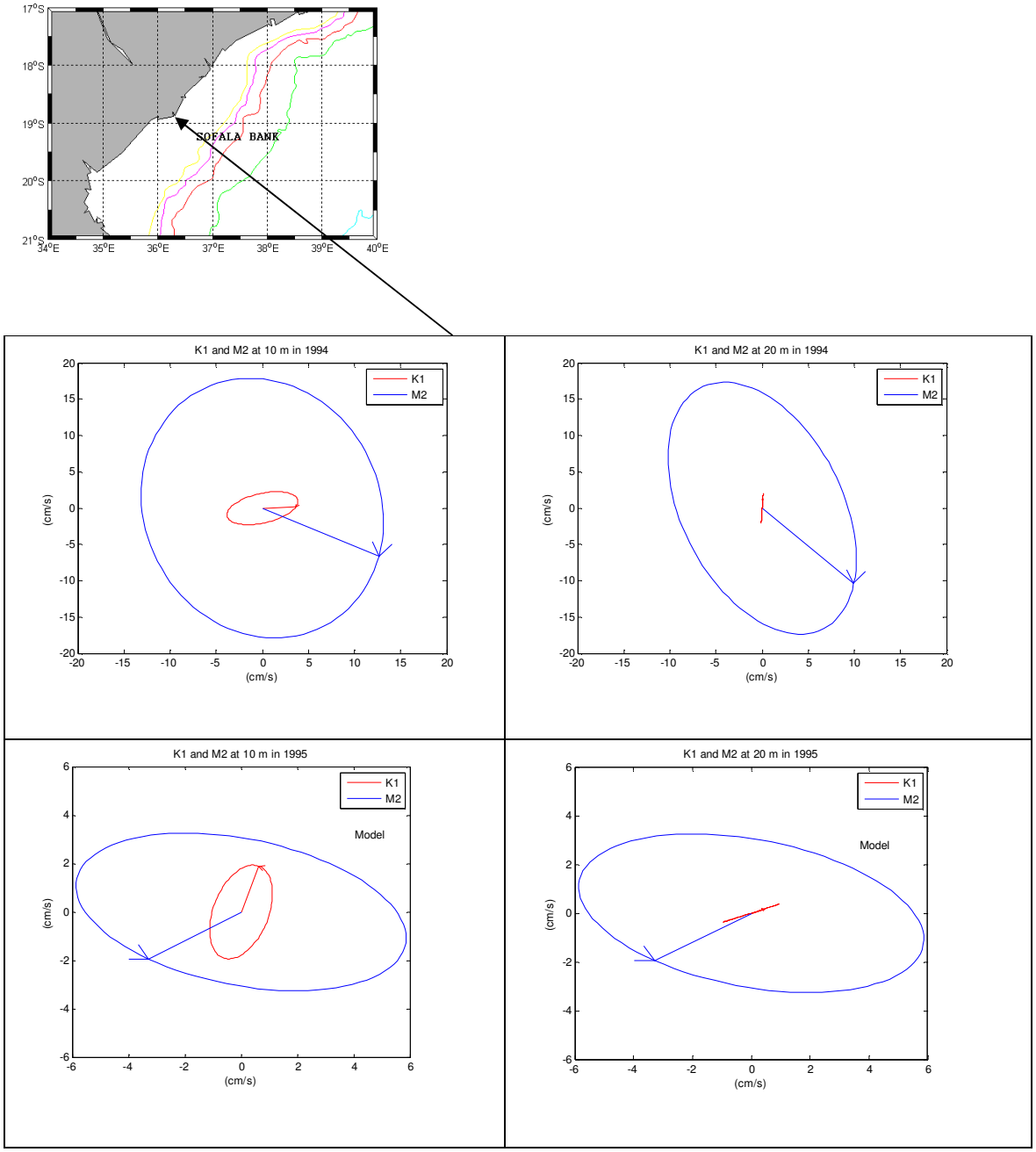

Figure 4.2: Tidal ellipses for K1 and M2 constituents observed (1994) and modeled (1995) at Sofala 94 location.

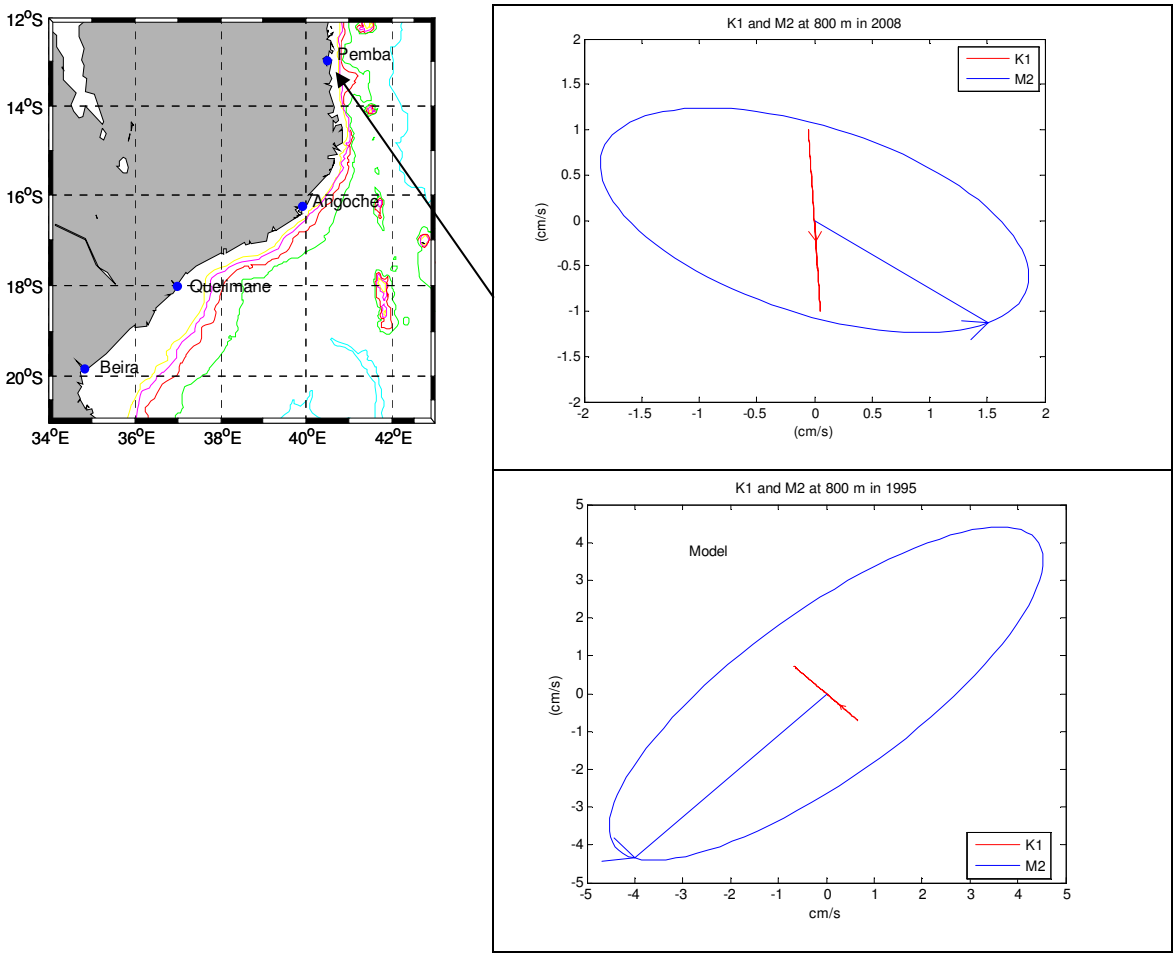

Figure 4.3: Tidal ellipses for K1 and M2 constituents observed (2008) and modeled (1995) at Pemba location.

4.3. Tidal amplification mechanism

Generally, in deep ocean tides elevations are usually small and tidal currents are weak. The astronomical forces have as input a high proportion of the tidal energy and distributed to the shelf in the form of a tidal energy flux. The tides are typically much larger and are the main source of mechanical energy on the shelf where a larger amount is dissipated from deep ocean (Simpson, 1998). The tide is amplified on the shelf, see Fig. 4.4. Change in depth, typically from 4000 m to about 100 m will cause the reduction in its phase velocity and wavelength. In order to maintain the energy flux, the energy density, and therefore the wave amplitude, must increase as the group velocity decreases. The group velocity is equal to the phase velocity ($c = \sqrt{gh}$) for long waves, where g is the gravity. The energy flux may be calculates

as $FLUX = \frac{1}{2}\rho g a^2 c$, where is the wave amplitude. If we assume the energy flux constant, $\frac{1}{2}\rho g a_1^2 c_1 = \frac{1}{2}\rho g a_2^2 c_2$, the amplitude changes for a depth change from h_1 to h_2 which gives (4.1).

$$\left(\frac{a_2}{a_1}\right)^2 = \left(\frac{h_1}{h_2}\right)^{1/2} \quad (4.2) \qquad \text{(from Simpson (1998); his formula 1).}$$

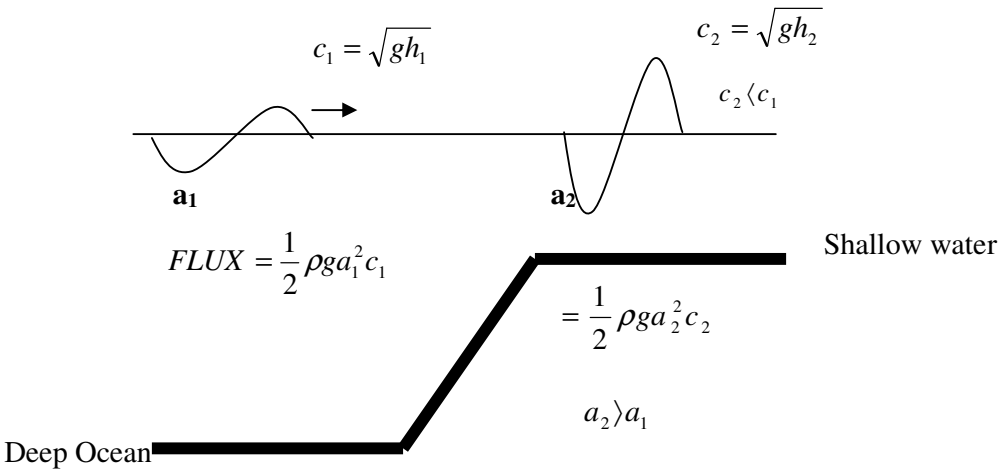

Figure 4.4: Tidal amplification mechanism, change in wavelength and group velocity.

If we consider h_1 = 4000 m and h_2 =100 m then the amplitude will increases for a progressive wave with a factor of 2.51 (from formula 4.2). It assumes that all energy incident from the deep ocean moves to the shelf without reflection (Simpson, 1998).

Table 4.1. Tidal amplification mechanism.

Station	Depth (m)	Obs. amplitude (m)	Observed ratio of amplitude (a_2/a_1)			Theoretic ratio of amplitude (a_2/a_1) (Eq.4.2.)		
			Sof94	Sof87	Pemb08	Sof94	Sof87	Pemb08
Sof94	25	1.23	X	1.3	1.3	X	1.7	2.5
Sof87	200	0.94	X	X	1.0	X	X	1.5
Pemb08	954	0.96	X	X	X	X	X	X

Calculation of ratio of amplitude (a_2/a_1) form formula 4.2 is depending of the depth which we consider as deep ocean and shallow water. This means that the ratio of amplitude will varies in accordance with depth of deep ocean and shallow water. Table 4.1 revealed that there is the difference between observed and theoretic ratio of amplitude. The biggest values are found in theoretical ratios of amplitude that is in Pemba which is much high. Looking to the table 4.1,

there is the indication that the tide does not behave as a progressive wave. The theoretical result for Pemba is much high comparing with Sof87 and Sof94.

4.4. Tidal mixing and water masses characteristics

Brown et al (1999) used the empirical relationship (Eq. 4.3) to predict whether or not a front in particular location.

$P = H / U^3$ (4.3) (from Brown et al (1999); their formula 8.1)

Where P represents a factor that turbulent mixing caused by tidal currents interacting with the sea-bed will extend to the surface. H is a water depth and U is the mean maximum surface tidal current speed. If P=50 the water column will be well mixed and for P=100 the water column will be stratified.

Between mixed and stratified waters there is the boundary or front which depends on the efficiency of the mixing. The strong horizontal temperature gradients between warmer surface water and cooler surface water define the frontal boundary (Pugh, 2004).

We choose the tidal velocity U as a function of bottom depth H to apply from the data (RCM7 in 1987 and RCM7 in 1994) as a linear function $U = \frac{\Delta U}{\Delta H} H + U_0$ (4.4)

Using the depth values from the CTD information was U calculated as a function of H:

$U = \frac{U_{200} - U_{25}}{200 - 25} H + U_0$, where U_{200} = 40 and U_{25} = 27 it will be $U = \frac{13}{175} H + 27$; the values are taken from table 2.8. With this distribution of U, P was calculated according to Eq. (4.3), and the results are shown in Fig 4.5 which shows the horizontal distribution of P. The value P=50 indicates a well mixed water column along the shelf (in dark blue color), the fronts (in blue color) that are typically zones of transition relatively sharp than boundaries and the stratified waters (P=100) which is representing by light blue to red color). Water depth and partly tidal current regime determine the position of the fronts. Comparison between Fig. 4.5 and Fig. 3.7b (see section 8 and 9) illustrates the same results. Mixing is found on the shelf and stratification offshore. Looking to the position of P (Fig. 4.5) and comparing with the salinity sections in Fig. 3.7b it compares quite well. We note that in section 8 the 4 innermost stations are well mixed and in section 10 only the two innermost stations are well mixed and

these positions seem to be close to P=50. The P=100 line is only slightly more offshore, and this also compares well with Fig. 3.7b, it seems that the stratification is developed around the shelf brake, see section 8.

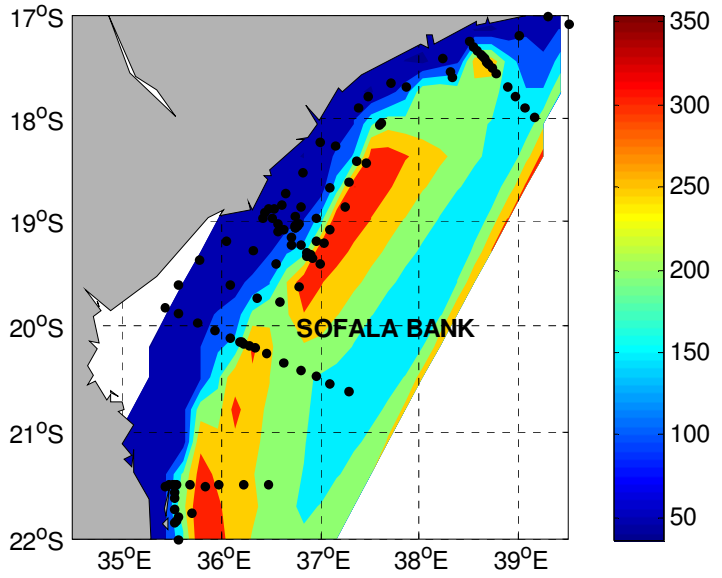

Figure 4.5: Horizontal distribution of the empirical mixing parameter P, see Eq. (2). P=50 indicates a well mixed ocean and P=100 a stratified ocean.

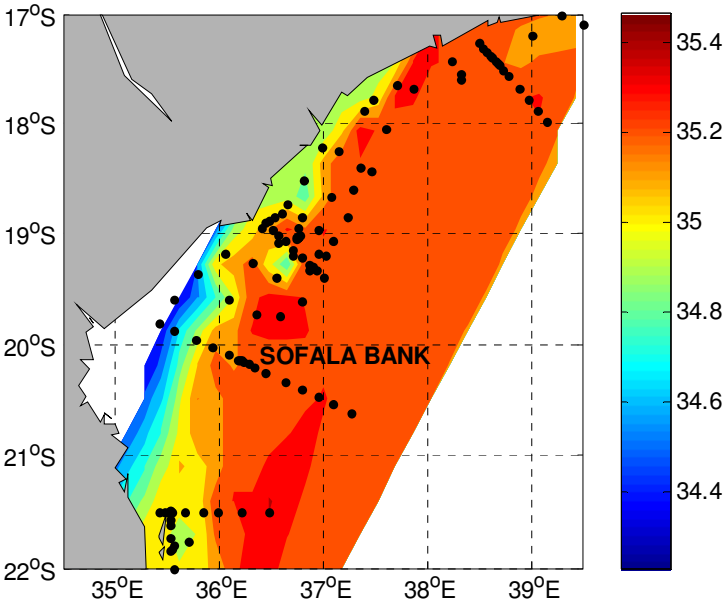

Figure 4.6: Horizontal distribution of salinity at 5 m depth at Sofala Bank.

Horizontal distribution of salinity at 5 m depth (Fig. 4.6) shows the influence of the Zambezi River water that moves from the shelf to the offshore. It is indicated by core of low salinity, about 34.8 psu (green color). The mixed water column is slightly and located on the shelf. When we move from the coast we find the stratification, which is more pronounced.

4.5. Nature of tidal waves

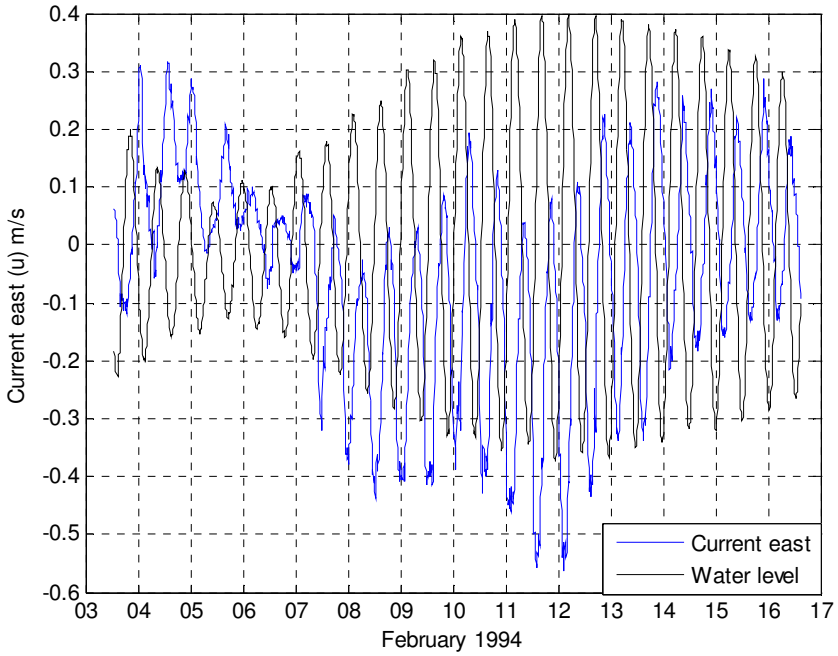

Figure 4.7: Water level and current in east direction at Sofala Bank.

During this study was chosen one mooring located in Sofala Bank (at Quelimane) in order to research which type of waves is possible to find in Mozambique Coast. For this comparison of water level and current speed towards east (u), given in Fig. 3.3 are plotted together in Fig.4.7. While progressive waves are characterized with maximum speed occurring at extreme water levels, for standing waves have maximum velocities when the rate of change of water level occurs. An inspection of Fig. 4.7 indicates that most of the time the tide has the structure of a standing wave. The result presents standing waves which are sum of two waves travelling in opposite directions (Brown et al, 1999 and Pugh, 2004). Where the water level is high we find the low current speed. Pugh (1987) concluded the fact that in Mozambique Channel there is a standing wave system. Gammelsrød and Hoguane (1995) also suggested

the existence of standing waves characteristics after analyze onshore offshore strong tidal signal of the mooring observation at the 60m depth at Sofala Bank 1987.

Pugh (2004) presented the calculation of angular speeds per hour. From it the phase difference between Maputo and Pemba is roughly one hour, see table 3.2. Using the formula for phase speed of a standing wave $\mathbf{c} = \sqrt{gh}$ and using the max depth of the Mozambique Channel, h= 4000 m we found that the maximum c= 200 m/s. This means that the wave will travel maximum 200 m/s*3600 s = 720 km in one hour, while the distance from Maputo to Pemba is almost the double. So this provides even another indication that the tides are standing waves in the Mozambican Channel.

5. Conclusions

Motivated by the description of tidal structures and mixing; and description of tidal currents along the Mozambique Coast, this thesis explored tides, currents and CTD data of Sofala Bank covered the years 1987, 1994, 1995, 2007 and 2008. Relationship between tides and currents variation were investigated in search of possible structures representative in each place. Following the questions raised in the introduction, the main findings are:

- There is the difference of amplitude in coastal stations (Fig.3.1c). The amplitude is high in Beira and is followed by Quelimane, Pemba and Maputo. Maputo and Beira demonstrates some delay relatively Quelimane and Pemba. The water level reaches at first Pemba followed by Quelimane, Maputo and Beira. The water levels amplitudes for coastal stations present the biggest (1.81 m) tidal component (M2) in Beira, see table 3.2. It is followed by Quelimane, Pemba and Maputo. The moorings results give the same impression. It shows the maximum (1.22 m) tidal component (M2) in Sofala 94 followed by Pemba 08 and Sofala 87, see table 3.2 and 3.3. Note that the mooring at Sofala 87 was anchored far from the coast (see Fig. 1.1) and at 200 m depth that induced the reduction of water level amplitude. In table 3.2 and 3.3 we note that the dominating tidal component (M2) is of the same order of magnitude for the coastal stations and the moorings. The maximum mooring M2 component was found at the most shallow mooring, namely the Sofala 94 anchored at 25 m depth, and for coast stations we found the maximum M2 component in Beira.
- Our findings indicate that tides along the Mozambican coast are standing waves. For instance we found (table 4.1) that the tides do not obey the tidal amplification mechanism (Simpson, 1998) valid for progressive waves. Also the lack of phase differences along the coast, see Fig.3.1c and the fact that the tidal current seem to be maximum when the water level is close to zero level, characteristic for standing waves, see Fig. 4.7 also support this hypothesis.
- The tidal currents patterns according to Fig. 4.1, 4.2 and 4.3 we notice that the dominating M2 component presents the biggest major axis of ellipse in Sofala 87 mooring anchored at 60 m depth, see also table 3.4. The component M2 for Sofala 87 and Pemba 08 mooring presents the same orientation of tidal ellipse that was anti-clockwise, except for Sofala 94 mooring, which was clockwise orientation.
- The water level amplitudes vary depending of location in coastal stations (table 3.1). The highest amplitude is found in Beira. The water level amplitudes of coastal stations

show some difference with ROMS model. And again; it seems due to the fact that the coastal stations were located at surface and the model at 30 m depth. The model shows the same structure of water level comparing with Sofala 94 mooring, although the model presents smaller amplitudes (low to a factor 1.3) than observations (Fig. 3.6). The water level amplitudes happen at almost same time for Sofala 94 mooring and model. The ROMS model performed well the patterns of tide variations comparing with Sofala 94 than with coastal stations. There is difference of tidal ellipses between mooring and model that shows the big major axis for observation except at 170 m and 800 m depth, which the observation has small major axis than model (table 3.4). Tidal ellipses of the mooring and model show that the component M2 has the same orientation (anti-clockwise), except for Sofala 94 mooring.

- Tides generate currents that interact with bottom producing turbulence, which tends to mix lower layers (Brown et al, 1999). In areas where the water is shallow and the tidal currents are strong enough the vertical mixing of the water column is extended and in other areas where the water is deeper and the tidal currents are weaker, less mixing occurs, and stratification (Brown et al, 1999). Our finding indicated that the stronger tidal current was observed in Sofala 87 mooring (table 3.4) and further a strong mixing is observed (Fig. 4.5). The shallow positions along the coast indicated the well mixed (P=50); and more offshore indicated the stratification (P=100). The salinity sections shown in Fig. 3.7b also presented the innermost stations well mixed, it seems that the stratification is developed around the shelf brake, see section 8. The influence of the brackish water on the shelf indicates a strong mixing on the shelf because the salinity is well mixed.

6. References

Brown et al (1999). *Waves, Tides and Shallow-water processes*. The Open University, pp 227.

Colling (2001). *Ocean Circulation*. The Open University, pp 286.

Gammelsrød, T. and Hoguane, A. (1995). *Water Masses, Currents and tides at Sofala Bank, November 1987*. Revista de Investigação Pesqueira, nº 22, pp 59.

Garrison, T. (1996). *Oceanography. An Invitation to Ocean Sciences*. Wadsworth Publishing Company, pp 538.

INAHINA (1995). *Tabela de marés*. República de Moçambique, pp 183.

Kaehler, S. et al (2008). *Preliminary Cruise Report N° 8/2008*. 2008 ASCLME Survey N° 4.

Lutjeharms, J. R. E. (2006b). *The coastal oceans of South-Eastern Africa*. In Robinson, A. and Brink, K. editors. Harvard University Press, Cambridge, MA. The sea, Volume 14B, pp 783-834.

Mann, K. & Lazier, J. (2006). *Dynamics of Marine Ecosystems*. Blackwell Publishing, pp 496.

Pinet, R. (2006). *Invitation to oceanography*. Jones and Barlett, pp 594.

Pond, S. and Pickard, G. (1983). *Introductory Dynamical Oceanography.* Elsevier Ltd Publishing, pp 329.

Pugh, D. (1987). *Tides, Surges and Mean Sea Level.* Bath Press, Avon, pp 443.

Pugh, D. (2004). *Changing Sea Levels.* Cambridge, pp 265.

Quartly, G. and Srokosz, M. (2004). *Eddies in the Southern Mozambique Channel*. Deep Sea Research Part II: Topical Studies in Oceanography, Volume 51, Pages 69-83.

Sætre, R. and Jorge da Silva, A. (1982). Water *masses and circulation of the Mozambique Channel*. Revista de Investigação pesqueira, pp 83.

Segtnan, O. (2006). *Simulating the circulation in the Mozambique Channel by use of a numerical ocean model*, s.e. Thesis, pp 72.

Sete, C. et al (2002). *Seasonal variation of tides, currents, salinity and temperature along the coast of Mozambique*, UNESCO (IOC) – ODINAFRICA, pp 72.

Simpson, A. (1998). *Tidal processes in Shelf Seas.* In Brink, K. and Robinson, A. Editors. The global Coastal Ocean: Processes and Methods. The sea, Volume 10, pp 150.

http:// www.aadi.no/Aanderaa/Document%20Library/1/.../Seaguard®%20**RCM**.pdf

http:// www.ess.co.at/ICZM/roms.html

http://www.icsm.gov.au/tides/SP9/links/AanderaaRCM7.html